

This discussion paper is/has been under review for the journal Atmospheric Chemistry and Physics (ACP). Please refer to the corresponding final paper in ACP if available.

Potential climate forcing of land use and land cover change

D. S. Ward¹, N. M. Mahowald¹, and S. Kloster²

¹Earth and Atmospheric Science, Cornell University, Ithaca, New York, USA

²Land in the Earth System, Max Planck Institute for Meteorology, Hamburg, Germany

Received: 13 April 2014 – Accepted: 26 April 2014 – Published: 14 May 2014

Correspondence to: D. S. Ward (dsw25@cornell.edu)

Published by Copernicus Publications on behalf of the European Geosciences Union.

Potential climate
forcing of land use
and land cover
change

D. S. Ward et al.

Title Page

Abstract

Introduction

Conclusions

References

Tables

Figures

⏪

⏩

◀

▶

Back

Close

Full Screen / Esc

Printer-friendly Version

Interactive Discussion

Abstract

Pressure on land resources is expected to increase as global population continues to climb and the world becomes more affluent, swelling the demand for food. Changing climate may exert additional pressures on natural lands as present day productive regions may shift, or soil quality may degrade, and the recent rise in demand for biofuels increases competition with edible crops for arable land. Given these projected trends there is a need to understand the global climate impacts of land use and land cover change (LULCC). Here we quantify the climate impacts of global LULCC in terms of modifications to the balance between incoming and outgoing radiation at the top of the atmosphere (radiative forcing; RF) that are caused by changes in long-lived and short-lived greenhouse gas concentrations, aerosol effects and land surface albedo. We simulate historical changes to terrestrial carbon storage, global fire emissions, secondary organic aerosol emissions, and surface albedo from LULCC using the Community Land Model version 3.5. These LULCC emissions are combined with estimates of agricultural emissions of important trace gases and mineral dust in two sets of Community Atmosphere Model simulations to calculate the RF from LULCC impacts on atmospheric chemistry and changes in aerosol concentrations. With all forcing agents considered together, we show that 45 % (+30 %, -20 %) of the present-day anthropogenic RF can be attributed to LULCC. Changes in the emission of non-CO₂ greenhouse gases and aerosols from LULCC enhance the total LULCC RF by a factor of 2 to 3 with respect to the LULCC RF from CO₂ alone. This enhancement factor also applies to projected LULCC RF, which we compute for four future scenarios associated with the Representative Concentration Pathways. We calculate total RFs between 1 to 2 W m⁻² from LULCC for the year 2100 (relative to a preindustrial state). To place an upper bound on the potential of LULCC to alter the global radiation budget we include a fifth scenario in which all arable land is cultivated by 2100. This “worst-case scenario” leads to a LULCC RF of 4.3 W m⁻² (± 1.0 W m⁻²), suggesting that not only energy policy but

Potential climate forcing of land use and land cover change

D. S. Ward et al.

Title Page

Abstract

Introduction

Conclusions

References

Tables

Figures



Back

Close

Full Screen / Esc

Printer-friendly Version

Interactive Discussion



land cover change began centuries before 1850, but at smaller rates (Pongratz et al., 2009). We compare the RF of LULCC to the RFs of other anthropogenic activities, which are dominated by fossil fuel burning.

The global LULCC RF and associated climate response are often portrayed as a balance between cooling biogeophysical effects (changes in surface energy and water balance) and the warming biogeochemical effect of increases in atmospheric CO₂ (e.g. Claussen et al., 2001; Brovkin et al., 2004; Foley et al., 2005; Bala et al., 2007; Cherubini et al., 2012). Claussen et al. (2001) found that the cooling from biogeophysical effects of land cover change dominated over the warming from associated CO₂ emissions in high-latitude regions where the land may be snow covered for part of the year, whereas tropical LULCC leads to a warming due to a weaker albedo forcing. This regional contrast in the dominant forcing from deforestation also applies to natural forest disturbances (O'Halloran et al., 2011). On a global scale, model estimates have shown nearly canceling climate responses to historical land cover change biogeophysical effects and CO₂ emissions (Brovkin et al., 2004; Sitch et al., 2005) and a small net warming (0.15 °C) from the same effects (Matthews et al., 2004).

These comparisons are highly uncertain in part because reports of historical CO₂ emissions from LULCC cover a wide range of values and are computed with several different methodologies (Houghton et al., 2012; Brovkin et al., 2013). Houghton (2010) estimates that 156 Pg carbon (C) has been emitted by historical LULCC from 1850 to 2005, using an inventory-based method (Houghton et al., 1983, 1999). This approach does not account for the feedback between increasing atmospheric CO₂ and LULCC C emissions, also known as the fertilization feedback (Arora and Boer, 2010), or for the diminished capacity of deforested land to act as a CO₂ sink as atmospheric CO₂ concentrations increase (Strassmann et al., 2008). Alternatively, LULCC C emissions are estimated with model simulations of the terrestrial biosphere with and without LULCC after assessing the difference in C stocks between the two simulations. With this approach the effects of CO₂ fertilization on LULCC C emissions can be accounted for, although there is as yet no consistent method for including feedbacks without using

Potential climate forcing of land use and land cover change

D. S. Ward et al.

Title Page

Abstract

Introduction

Conclusions

References

Tables

Figures

⏪

⏩

◀

▶

Back

Close

Full Screen / Esc

Printer-friendly Version

Interactive Discussion



Potential climate forcing of land use and land cover change

D. S. Ward et al.

Title Page

Abstract

Introduction

Conclusions

References

Tables

Figures

⏪

⏩

◀

▶

Back

Close

Full Screen / Esc

Printer-friendly Version

Interactive Discussion

5 a fully-coupled carbon cycle model (Arora and Boer, 2010). Gasser and Ciais (2013) propose a framework by which some of these studies may be compared. The results of several studies that calculate a LULCC C flux are summarized by Houghton (2010) and Pongratz et al. (2009). They report a range of previously published C emission estimates for LULCC of 138 PgC to 294 PgC for years 1700 to 2000, including results from the modeling studies of Strassmann et al. (2008) and Shevliakova et al. (2009). Strassmann et al. (2008) account for the impact of CO₂ fertilization and estimate that this negative feedback on C emissions amounts to roughly 25 % of the LULCC C flux. More recently, Lawrence et al. (2012) calculated a net LULCC C flux of 128 PgC for 10 1850 to 2005, and Ciais et al. (2013) suggested a range of 180 ± 80 PgC for the time period 1750 to 2011. Arora and Boer (2010) estimate a substantially smaller historical LULCC C flux between 40 and 77 PgC using a coupled climate-carbon cycle model. Although, the representation of nitrogen-limitation on plant growth, not included in Arora and Boer (2010), may lead to a greater LULCC C flux in otherwise similar model experiments (Arora et al., 2013).

15 Model estimates of C emissions from soils that have been disrupted by land use are poorly constrained (Houghton, 2010) and introduce major uncertainty into estimates of the LULCC C flux (House et al., 2002). In a review of field studies, Guo and Gifford (2002) conclude that soil C is increased for most conversions of natural land to pasture, and decreased for conversions to cropland. Lal (2004) estimates that cultivation 20 has caused the loss of 78 ± 12 PgC from soils since 1850. Modeling studies suggest that LULCC can cause a net loss of soil C globally, from ~ 13 % of total LULCC C emitted (Strassmann et al., 2008) to ~ 37 % (Shevliakova et al., 2009), or a net gain as in Arora and Boer (2010). In addition, there is a potentially major source of CO₂ 25 from deforestation and forest degradation in tropical peat swamp forests that has only recently been recognized (Hergoualc'h and Verchot, 2011).

Previous studies have shown that land cover change also modifies climate by biogeophysical effects such as changes to surface latent and sensible heat fluxes and to the hydrological cycle (DeFries et al., 2002; Feddema et al., 2005; Brovkin et al.,

Potential climate forcing of land use and land cover change

D. S. Ward et al.

Title Page

Abstract

Introduction

Conclusions

References

Tables

Figures

⏪

⏩

◀

▶

Back

Close

Full Screen / Esc

Printer-friendly Version

Interactive Discussion

2006; Pitman et al., 2009; Lawrence and Chase, 2010). In general, while important for local or regional climate especially in the tropics (Strengers et al., 2010), these effects are considered minor on a global scale (Lawrence and Chase, 2010) and are difficult to quantify using the RF concept (Pielke et al., 2002). Of these biogeophysical effects of LULCC, land albedo change is recognized as the dominant forcing globally (Betts et al., 2007; Pongratz et al., 2009). The surface underlying a forest may have a different albedo than the canopy that is revealed following forest removal. In high latitude forests, clear-cut areas may become snow-covered in the winter and therefore, highly reflective. Many estimates of the global RF of land albedo change have been published, derived from modeling experiments (e.g. Brovkin et al., 1999, 2004; Betts, 2001; Defries et al., 2002; Betts et al., 2007; Davin et al., 2007; Pongratz et al., 2009; Skeie et al., 2011; Lawrence et al., 2012; Avila et al., 2012) and from satellite retrievals (Myrhe et al., 2005). In all these studies, a representation of the present day land albedo, whether simulated or observed by satellite, is compared to the land surface albedo with preindustrial vegetation, or the potential vegetation. Estimates for the global albedo change RF range from -0.10 W m^{-2} (Skeie et al., 2011) to -0.28 W m^{-2} (Lawrence et al., 2012), with a central estimate from the IPCC of -0.20 W m^{-2} (Forster et al., 2007). The inhomogeneous distribution of forcing from surface albedo changes and short-lived trace gas and aerosol species could lead to non-additive (A. D. Jones et al., 2013), and highly variable local climate responses (Lawrence et al., 2012). Therefore, we use the RF for our assessment of global-scale climate impacts and acknowledge the limits of the RF concept for predicting the diverse and local impacts of land use (Betts, 2008; Runyan et al., 2012).

Additional LULCC forcings are often grouped in with fossil fuel burning and other activities for assessment of the anthropogenic RF (e.g. Forster et al., 2007). Nevertheless, there is some recognition of the importance of evaluating LULCC emissions of non- CO_2 greenhouse gases separately from fossil fuel emissions for targeting emission reduction policies (Tubiello et al., 2013). Less attention is given to forcings from short-lived atmospheric species that are affected by LULCC. Foley et al. (2005) ac-

Potential climate forcing of land use and land cover change

D. S. Ward et al.

Title Page

Abstract

Introduction

Conclusions

References

Tables

Figures

⏪

⏩

◀

▶

Back

Close

Full Screen / Esc

Printer-friendly Version

Interactive Discussion

knowledge that changes in the concentrations of short-lived species, aerosols and O₃, from LULCC are important for air quality assessment but do not estimate the impacts of these species on climate. Unger et al. (2010) partition sources of global, anthropogenic RF into economic sectors, including agriculture. They consider non-CO₂ greenhouse gas and aerosol forcing agents but only for present day land use emissions and they do not include land cover change. The full contribution of LULCC to global RF compared to the contribution from other anthropogenic activities remains unquantified.

Here we compute the CO₂ and albedo RF from global LULCC and compare to previous estimates of these values, but we also compute the global LULCC RF from non-CO₂ greenhouse gases (CH₄, N₂O, O₃), and aerosol effects (direct, indirect, deposition on snow and ice surfaces). Individual forcings are computed from the results of terrestrial model simulations forced with historical land cover changes and wood harvesting, and projected land cover changes from five future scenarios. Because the land model used here includes a carbon model, fire module and emissions of volatile organic compounds, we can uniquely account for the complicated interplay between land use and fire (e.g. Marlon et al., 2008; Kloster et al., 2010; Ward et al., 2012). Four of the future scenarios of land cover change correspond to the four Representative Concentration Pathways (RCP) that were developed for the Climate Model Intercomparison Project in preparation for the IPCC 5th assessment report (AR5) (Lawrence et al., 2012; Hurtt et al., 2011; van Vuuren et al., 2011). The low emissions scenario, RCP2.6, includes widespread proliferation of bioenergy crops, while RCP4.5 is characterized by global reforestation as a result of carbon credit trading and emission penalties (Hurtt et al., 2011). The higher emissions scenarios include expansion of crop area at the expense of existing grasslands (RCP6.0; Fujino et al., 2006) or forests (RCP8.5; Riahl et al., 2007; Hurtt et al., 2011). We introduce a fifth, worst-case scenario, in which all arable and pasturable land is converted to agricultural land, either for crops or pasture, by the year 2100. The worst case scenario was not developed within an integrated modeling framework and, therefore, its likelihood of occurrence given economical and additional environmental constraints is difficult to judge. Instead, this scenario gives a theoretical

We use the Ramankutty et al. (2002) definitions for soil pH, soil carbon, defined as the mass of C per meter squared in the top 30 cm of the non-gravel soil, and for GDD, defined as the number of °C by which daily mean temperature exceeds 5 °C.

For the moisture index we use the Climate Moisture Index (CMI) (Willmott and Fedema, 1992) which is defined using precipitation, P , and potential evaporation, PE, data as:

$$\begin{aligned} \text{CMI} &= 1 - \text{PE}/P \quad \text{when } P \geq \text{PE} \\ \text{CMI} &= P/\text{PE} - 1 \quad \text{when } P < \text{PE} \\ \text{CMI} &= 0 \quad \text{when } P = \text{PE} = 0 \end{aligned} \quad (1)$$

We use 1979–2009 averages for climate variables and year 2000 crop area data (Ramankutty et al., 2008). For fitting the individual sigmoidal curves, we restrict the data to only those points that are otherwise optimal for crops, as in Ramankutty et al. (2002). For example, when fitting the CMI data, we restrict the crop area data to regions where the GDD, soil C, and soil pH support crops. This isolates grid points that could be CMI limited.

Following Ramankutty et al. (2002), we fit a single sigmoidal curve to the GDD data, and the CMI data, a double sigmoidal curve to the soil C data and explicitly define a pH limit function. The expressions for these functions from Ramankutty et al. (2002) are given below with new coefficients computed for our study:

$$f_1(\text{GDD}) = \frac{1}{[1 + e^{a(b-\text{GDD})}]} \quad (2)$$

$$f_2(\alpha) = \frac{1}{[1 + e^{c(d-\alpha)}]} \quad (3)$$

Where $a = 0.0037$, $b = 1502$, $c = 10.16$, and $d = 0.3544$.

$$g_1(\text{C}_{\text{soil}}) = \frac{a}{[1 + e^{b(c-\text{C}_{\text{soil}})}]} \frac{a}{[1 + e^{d(h-\text{C}_{\text{soil}})}]} \quad (4)$$

Potential climate forcing of land use and land cover change

D. S. Ward et al.

Title Page	
Abstract	Introduction
Conclusions	References
Tables	Figures
◀	▶
◀	▶
Back	Close
Full Screen / Esc	
Printer-friendly Version	
Interactive Discussion	



Where $a = 22.09$, $b = 3.759$, $c = 1.839$, $d = 0.0564$, and $h = 106.5$.

$$g_2(\text{pH}_{\text{soil}}) = \begin{cases} -1.64 + 0.41\text{pH}_{\text{soil}} & \text{if } \text{pH}_{\text{soil}} \leq 6.5 \\ 1 & \text{if } 6.5 < \text{pH}_{\text{soil}} < 8 \\ 1 - 2(\text{pH}_{\text{soil}} - 8) & \text{if } \text{pH}_{\text{soil}} \geq 8 \end{cases} \quad (5)$$

These functions are multiplied together to create suitability indices: the product of the f functions gives the climate suitability index and the product of the g functions gives the soil suitability index. Natural land that is “suitable” for crops based on these criteria is converted to cropland (on a linear year-to-year basis) between years 2006–2100. We assume area that is suitable for crops based on climate, but not soil characteristics, can support grass and is used for pasturing animals. This assumption leads to the replacing of most tropical forests by crops or grasslands. The global potential crop area computed here for present day climate is 4180 Mha and the potential pasture area is 3110 Mha, compared to reported year 2010 utilized areas of 1570 Mha for crops and 2030 Mha for pasture (Hurt et al., 2011). Since the potential crop area depends on climate, it is likely to change in the future. One estimate, using a business-as-usual greenhouse gas emissions scenario, yields a 16% increase of the 1961–1990 potential crop area by 2070–2099, mainly in high latitudes (Ramankutty et al., 2002). We did not include climate-dependent trends in potential crop area in this study but note here that doing so may increase the year 2100 RF of the worst case scenario LULCC. Further information on how the potential crop and pasture area is translated into LULCC is given in Sect. 3.1.1. As discussed below, emissions of CH_4 and N_2O from agriculture in the worst case scenario are based on emissions of these gases per area of crop/pasture in the RCP8.5 scenario and scaled by the differences in crop and pasture area between RCP8.5 and the worst case scenario. We do not consider possible future changes in natural emissions of CH_4 and N_2O . Other calculations are done similarly to the RCPs, as discussed below in Sect. 3.

Potential climate forcing of land use and land cover change

D. S. Ward et al.

Title Page

Abstract

Introduction

Conclusions

References

Tables

Figures

⏪

⏩

◀

▶

Back

Close

Full Screen / Esc

Printer-friendly Version

Interactive Discussion



3 Methods: radiative forcing calculations

Our approach to computing the RFs begins with estimating emissions of trace gases and aerosols from a diverse set of LULCC activities, many of which are illustrated schematically in Fig. 1. We model the following LULCC activities with a global terrestrial model; wood harvesting, land cover change, and changes in fire activity, including deforestation fires. Changes in the terrestrial model carbon cycle driven by the historical and projected LULCC are used to derive the RF of surface albedo change, and emissions of CO₂, SOA, smoke, and mineral dust from LULCC. We assemble emissions from additional LULCC activities; agricultural waste burning, rice cultivation, fertilizer applications, and livestock pasturage, from available datasets corresponding to the RCP LULCC projections. Altogether, we consider LULCC emissions of non-methane hydrocarbons (NHMCs), NO_x, CH₄, N₂O, CO₂, NH₃, SOA, black carbon (BC), organic carbon (OC), SO₂, and mineral dust. From these emissions we calculate the change in concentrations of forcing agents between years 1850 to 2010 and 1850 to 2100 for all future projections. The different lifetimes of the forcing agents means that a single model approach cannot easily capture changes in all the forcing agents (Unger et al., 2010) and, therefore, a combination of models and methodologies are used here (Fig. 2). Note that RFs due to fossil fuels and other anthropogenic activities are calculated in this study for RCP4.5 emissions with identical methodology to that used for LULCC emissions.

Here we describe the methods for computing the various RFs, organized in four sections, corresponding to the rows in Fig. 2:

1. First the *LULCC activities* included in the analysis are outlined (Sect. 3.1).
2. This is followed by an explanation of the sources of the *emissions* data (Sect. 3.2).
3. Then the methods and models used to *compute concentration changes* are described (Sect. 3.3).
4. Next, the methods for *calculating the RFs* are explained (Sect. 3.4).

Potential climate forcing of land use and land cover change

D. S. Ward et al.

Title Page

Abstract

Introduction

Conclusions

References

Tables

Figures



Back

Close

Full Screen / Esc

Printer-friendly Version

Interactive Discussion



release of carbon that would otherwise occur by decomposition. Deforestation fires do, however, contribute small amounts of CH₄, N₂O, O₃ precursor gases, and aerosols to the atmosphere that would not have been released through decomposition.

Global burned area is reduced, both historically and in the future, by LULCC in our simulations (for RCP4.5, which includes large scale reforestation, the reduction is only a few percent and LULCC actually leads to a small increase in global fire emissions). This result matches our current understanding of the impact of LULCC on wildfires (Kloster et al., 2012; Marlon et al., 2008).

3.1.3 Agricultural activities

Additional emissions from LULCC activities associated with agriculture were taken from the integrated assessment model emissions for the different RCPs (e.g. van Vuuren et al., 2011) and are estimated based on RCP8.5 for the worst case scenario, as described below. These activities are fertilizer application, soil modification, livestock pasturage, rice cultivation and agricultural waste burning.

3.2 Emissions

This section describes the sources and accompanying computations for LULCC emissions of all relevant trace gas and aerosol species (Fig. 2). For non-LULCC related emissions (such as those from fossil fuel burning) we use the emission inventories from the Atmospheric Chemistry and Climate Model Intercomparison Project (ACCMIP) (Lamarque et al., 2010) for historical time periods, with future emissions from RCP4.5 (Wise et al., 2009). These datasets include emissions of non-methane hydrocarbons (NMHCs), NO, NH₃, SO₂, and organic carbon (OC) and black carbon (BC) aerosols.

Potential climate forcing of land use and land cover change

D. S. Ward et al.

Title Page

Abstract

Introduction

Conclusions

References

Tables

Figures

⏪

⏩

◀

▶

Back

Close

Full Screen / Esc

Printer-friendly Version

Interactive Discussion



to the carbon emissions from fires to determine the contribution of fires to the various chemical species (see Fig. 2) including NMHCs, CH₄, N₂O, NH₃, BC, OC, and SO₂ (Kloster et al., 2010; Ward et al., 2012). Fire emissions of BC and OC are reduced by 13% due to LULCC in year 2010 and reduced for projected LULCC in the year 2100, except for RCP4.5 (8% increase; Table 2).

3.2.3 Dust emissions

Agricultural activities have been linked to increased wind erosion of soils and greater dust emission in semi-arid regions (Ginoux et al., 2012). To address the impact of LULCC on dust emissions in our CAM simulations we introduce a modified soil erodibility dataset for each scenario. For each model grid box, a new soil erodibility value is set equal to the sum of the original soil erodibility and the fraction of the grid box that is cultivated land. We then introduce a parameter that weights the cultivated fraction in the soil erodibility computation such that the fraction of the dust flux resulting from cultivation in the year 2000 for eight regions (N. America, S. America, N. Africa, S. Africa, W. Asia, C. Asia, E. Asia, and Australia) is comparable to recently reported, satellite-derived values for each region (Ginoux et al., 2012). The weighting parameter for cultivated land was tuned with three iterations of four-year global atmospheric model simulations (using the a similar model setup to that described in Sect. 3.3.5), comparing the results for the tuned and un-tuned soil erodibility to the Ginoux et al. (2012) estimates for each region after each iteration. From this tuning we estimate reasonable weighting parameters for the cultivated fraction of land in each of the eight regions. The weighting parameters are applied to the timeseries of historical and projected crop area to create timeseries of soil erodibility that are modified by cultivation.

Ginoux et al. (2012) estimate that 25% of present day, global dust emissions are caused by anthropogenic activities. We estimate an increase in year 2010 global dust emissions from historical LULCC of about 20% (Table 2). Once these relationships between land use and dust are developed in the current climate, the natural dust source, along with changes in vegetation and climate are allowed to interact with the prognostic

Potential climate forcing of land use and land cover change

D. S. Ward et al.

Title Page

Abstract

Introduction

Conclusions

References

Tables

Figures



Back

Close

Full Screen / Esc

Printer-friendly Version

Interactive Discussion



dust scheme to predict changes in dust (Mahowald et al., 2006; Albani et al., 2014). The extreme expansion of crop and pasture area in the worst case scenario causes global dust emissions, from natural and human-impacted sources, to more than triple by the year 2100 using this methodology (Table 2).

3.2.4 SOA emissions

Biogenic emissions of isoprene, monoterpenes, carbon monoxide (CO) and methanol depend on leaf area index (LAI) and, therefore, also on LULCC. We compute biogenic trace gas emissions using an offline version of the Model of Emissions of Gases and Aerosols from Nature (MEGAN) (Guenther et al., 2006) with a forced diurnal cycle for temperature and solar radiation (Ashworth et al., 2010). The monthly average LAI output from CLM are used for each scenario to produce the biogenic emissions with LAI scaled globally such that predicted year 2000 isoprene emissions match present day global estimates from Heald et al. (2008).

Some biogenic NMHCs, notably monoterpenes and isoprene, can undergo gas to particle phase transitions in the atmosphere after oxidation (Heald et al., 2008) and contribute to changes in aerosol concentrations. The rate of secondary aerosol production depends on the concentrations of the gas precursors, but also the oxidation capacity of the troposphere (Shindell et al., 2009). Both criteria are predicted in our atmospheric chemistry model simulations, described in Sect. 3.3.1. Emissions of biogenic SOA precursors (mainly isoprene) are approximately unchanged by LULCC in the year 2010 but are reduced by projected changes in land cover for the future RCP between 6 to 16 % (Table 2). For comparison, Wu et al. (2012) calculate a ~ 10 % decrease in isoprene plus monoterpene emissions from LULCC between 2000 and 2100 using the IPCC A1B future emissions scenario.

Potential climate forcing of land use and land cover change

D. S. Ward et al.

Title Page

Abstract

Introduction

Conclusions

References

Tables

Figures



Back

Close

Full Screen / Esc

Printer-friendly Version

Interactive Discussion



3.2.5 CO₂ emissions

The anthropogenic contribution to the concentration of atmospheric CO₂, used to compute the RF at years 2010 and 2100, depends on the history of anthropogenic CO₂ emissions up to that point. We estimate yearly LULCC emissions to the atmosphere as being equivalent to the global annual change in terrestrial carbon storage due to LULCC. Therefore, sources as well as sinks of CO₂ associated with LULCC are accounted for in the CO₂ emissions.

LULCC emissions of CO₂, computed from the CLM simulations, are decreased in the simulations without changing land cover. Decreased atmospheric CO₂ will also lead to lower terrestrial carbon storage through the CO₂-fertilization feedback, but our simulations do not capture this feedback since we prescribe the same CO₂ forcing in CLM regardless of the LULCC. Arora and Boer (2010) show that this form of “double-counting” land carbon storage can lead to overestimates of 20th century LULCC carbon emissions (by $\sim 0.33 \text{ PgCyr}^{-1}$). However, a recent model intercomparison study suggested that including nitrogen (N)-limitation dramatically reduces terrestrial carbon pool sensitivity to changes in CO₂ concentration (Arora et al., 2013). Land carbon uptake in coupled models using the CN version of CLM was only 40 % as sensitive to changes in CO₂ concentration and surface temperature increases (known as the climate change feedback) compared to the model used by Arora and Boer (2010). Therefore we adjusted the yearly LULCC carbon emissions downward by 0.14 PgCyr^{-1} to account for the CO₂ fertilization feedback.

Other model parameters, including aerosol and biogenic NHMC fluxes, depend on LAI, which would also be impacted by the different CO₂ fertilization. However, due to the non-linearity of the aerosol and ozone response we do not apply an adjustment to these RFs but note here that the magnitude of the year 2010 aerosol, O₃ and indirect CH₄ RFs may be small overestimates.

Potential climate forcing of land use and land cover change

D. S. Ward et al.

Title Page

Abstract

Introduction

Conclusions

References

Tables

Figures

⏪

⏩

◀

▶

Back

Close

Full Screen / Esc

Printer-friendly Version

Interactive Discussion



3.2.6 N₂O emissions

N₂O has both industrial and agricultural sources, in addition to a large natural source from soils and oceans. Total anthropogenic N₂O emissions have been estimated for the historical time period and projected for RCP4.5 (Meinshausen et al., 2011a). Additional information regarding natural emissions and also agricultural emissions are needed to partition the anthropogenic N₂O emissions into LULCC and non-LULCC components and estimate the associated RFs. We follow the methodology of Meinshausen et al. (2011b) in which the N₂O budget is balanced for a historical time period to extract the natural emissions from the total anthropogenic emissions. Natural emissions of N₂O decrease from about 11 to 9 TgN (N₂O) yr⁻¹ using this method between the years 1850 and 2000. We maintain the year 2000 emissions, 9 TgN (N₂O) yr⁻¹, for the years 2000 to 2100. Future land cover change, particularly the worst case scenario, could lead to further decreases in natural N₂O emissions. However, not enough is known about global natural N₂O emissions to justify changing the future emission rate for this analysis (Syakila and Kroeze, 2011).

Anthropogenic emissions of N₂O have been partitioned into agricultural (LULCC) and other anthropogenic (primarily fossil fuel) sources, which have been further partitioned into animal production and cultivation sources for years prior to 2006 (Syakila and Kroeze, 2011). We compute the global N₂O emitted per area covered by crop or pasture in the year 2000 using these estimates. Our estimate for year 2010 N₂O emissions from agriculture, 4.3 TgN (N₂O) yr⁻¹, is at the lower end of previously reported values compiled by Reay et al. (2012), ranging from 4.2 to 7 TgN (N₂O) yr⁻¹. The year 2000 ratios of emission per area are applied to future changes in crop or pasture area to compute future LULCC N₂O emissions for all scenarios. This assumes no future trends in the rates per cultivated land area of the major agricultural N sources: N fertilizer application and animal waste management (Syakila and Kroeze, 2011). Our approach results in increased N₂O emissions from agriculture between years 2010 and 2100 for RCP2.6, RCP8.5, and the worst case scenario (Table 2). Emissions decrease

Potential climate forcing of land use and land cover change

D. S. Ward et al.

Title Page

Abstract

Introduction

Conclusions

References

Tables

Figures



Back

Close

Full Screen / Esc

Printer-friendly Version

Interactive Discussion



Potential climate forcing of land use and land cover change

D. S. Ward et al.

Title Page

Abstract

Introduction

Conclusions

References

Tables

Figures

⏪

⏩

◀

▶

Back

Close

Full Screen / Esc

Printer-friendly Version

Interactive Discussion



(year 2100) concentrations. We compare the concentration with all anthropogenic CH₄ sources/influences to the concentration with either LULCC or other anthropogenic sources/influences removed to compute the change in concentration for each case. The lifetime of CH₄ in the atmosphere (~ 9 years) means our simulations are too short to directly simulate the changes in CH₄ concentration. Instead we use approximations based on the known emissions of CH₄ and changes in the quick-adjusting main chemical sink for CH₄ – the hydroxyl radical (OH).

If we remove direct emissions of CH₄ from a particular source such as LULCC, a new steady state concentration can be approximated using the following expression from Ward et al. (2012):

$$\Delta[\text{CH}_4] = F \cdot \Delta E / E_0 \cdot [\text{CH}_4]_0 \quad (6)$$

such that a percentage change in CH₄ emissions, E , leads to a percentage change in concentration, $[\text{CH}_4]$, times the ratio of the perturbation lifetime to the initial lifetime, F . We do not calculate F from our simulations but use $F = 1.4$ as recommended by the IPCC (Prather et al., 2001).

Changes in global OH concentration can be used to approximate the change in CH₄ lifetime caused by a change in emissions (Naik et al., 2005). Here we use the OH concentrations predicted in the CAM4 simulations for each case. The impact of non-LULCC emissions on CH₄ lifetime is taken as the difference between the year 2010 or 2100, and year 1850 CH₄ lifetime in the simulations with no LULCC emissions. Estimated this way, the CH₄ lifetime decreases by more than two years between 1850 and 2010 and by one and a half years between 1850 and 2100.

We compute the change in concentration due to the change in CH₄ lifetime, τ , with respect to reaction with OH using this expression (Naik et al., 2005):

$$\Delta[\text{CH}_4] = F \cdot [\text{CH}_4]_0 \cdot \frac{\Delta\tau}{\tau_0} \quad (7)$$

Here we also use $F = 1.4$ to account for the positive feedback between CH₄ and OH (Naik et al., 2005).

3.3.3 CO₂ concentration

CO₂ is chemically inert in the atmosphere but, over time, the airborne fraction of emitted CO₂ decreases as ocean and land uptake of carbon occurs. Therefore, the most recent CO₂ emissions will have the highest airborne fraction. We apply a CO₂ pulse response function (Enting et al., 1994) to compute the airborne fraction of the yearly pulse emissions at the year 2010 or 2100, following previously used methods (e.g. Randerson et al., 2006; Ward et al., 2012). This weighting is especially important for non-LULCC emissions, which have been largest over the most recent decades.

3.3.4 N₂O concentration

Nitrous oxide is a long-lived greenhouse gas with a lifetime in the troposphere of over 100 years. Therefore, we use a simple atmospheric box model that can be run quickly for many model years to diagnose changes in N₂O concentration that result from LULCC and other anthropogenic emissions. The box model uses an expression of N₂O mass balance to predict changing concentrations, C , with time given yearly emissions, E , and a dynamic N₂O lifetime, τ (Kroeze et al., 1999):

$$\frac{dC}{dt} = \frac{E}{S} - \frac{C}{\tau} \quad (8)$$

Here, S is a conversion factor ($4.8 \text{ Tg N ppbv}^{-1}$) and t is time (years). The N₂O lifetime is dependent on its own concentration, which we account for here following Meinshausen et al. (2011b) and using a year 2000 reference state:

$$\tau = \tau_0 \left(\frac{C}{C_0} \right)^{-0.05} \quad (9)$$

We run the box model from simulation year 1850 through 2100 with natural and anthropogenic emissions, but with emissions from the source of interest, either LULCC or

other anthropogenic activities, removed. We assume that the decrease in natural N₂O emissions (Syakila and Kroeze, 2011) is attributable to LULCC. This decreases the net LULCC emissions of N₂O.

3.3.5 Aerosols concentrations

5 We use CAM version 5 (Liu et al., 2011) with the three-mode Modal Aerosol Model (MAM3) (Liu et al., 2012), including the two-moment microphysical scheme (Morrison and Gettelman, 2008) and aerosol/cloud interactions for stratiform clouds, to simulate aerosol dynamics on a global scale. The more recent version of CAM is used here, as opposed to CAM4, to allow use of MAM3, which is not available for CAM4. Unfortunately chemistry was not yet available in CAM5 at the time of this study, so that different versions of the model had to be run for chemistry and aerosols. Since we use CAM4 and CAM5 to model concentration changes for separate forcing agents (trace gases in CAM4 and aerosols in CAM5), differences in physics between the two models do not affect our results. CAM5 is setup with horizontal grid spacing of 1.9° latitude by 2.5° longitude with 26 vertical levels and a timestep of 30 min. Each simulation is branched from a two-year spinup using year 2000 climate conditions (air temperature, sea surface temperature, solar forcing, etc.). Model setup is identical for all simulations except for aerosol emissions, which are specific to the case (LULCC vs. no-LULCC, year 2010 vs. year 2100). In CAM5, aerosols are both radiatively and microphysically active. This enables simulation of aerosol indirect effects but leads to different model climates for different initial aerosol emissions. To isolate the impacts of aerosols on the RF we integrate CAM5 for four years post-spinup and use the annual average for analysis. This smooths out the interannual variability in the model climate state to minimize its impact on the RF (Wang et al., 2011).

Potential climate forcing of land use and land cover change

D. S. Ward et al.

Title Page

Abstract

Introduction

Conclusions

References

Tables

Figures

⏪

⏩

◀

▶

Back

Close

Full Screen / Esc

Printer-friendly Version

Interactive Discussion

3.4 RF calculations

We note here that all future LULCC RFs are calculated assuming background concentrations of trace gases and aerosols that are characteristic of RCP4.5. With this approach we can examine the impacts of the range in projected LULCC on RF independent of other anthropogenic activities. Although we are not able to report, for example, the RF of projected LULCC from the RCP8.5 scenario in the context of RCP8.5 fossil fuel emissions. Using a different projection to provide the background concentrations would modify the resulting LULCC RFs.

3.4.1 Tropospheric O₃

To assess the global mean RF of O₃ from the changes in emission of short-lived precursors and deposition, we compute radiative fluxes at the tropopause with the CAM4 output three-dimensional O₃ fields included, and also with tropospheric O₃ removed. This is accomplished by running the CAM4 radiation package offline with the Parallel Offline Radiative Transfer (PORT) tool (Conley et al., 2013). The difference in net radiative flux at the tropopause caused by removing O₃ gives the total RF of tropospheric O₃ in each case. The difference in O₃ RF between cases with LULCC and the corresponding case without LULCC is equivalent to the contribution from LULCC to the RF. The contribution of other anthropogenic activities is estimated by computing the difference between the year 2010 or 2100 simulations without LULCC, and the 1850 simulation without LULCC.

The short-lived O₃ RF estimated here is an instantaneous forcing since we do not allow for stratospheric temperature adjustment. Hansen et al. (2005) estimate a ratio of adjusted RF to instantaneous RF of approximately 0.8 in global simulations for the period between 1880 to 2000. We multiply the instantaneous RFs for O₃ by 0.8 to account for the stratospheric adjustment and report adjusted RFs.

Tropospheric O₃ acts as a source for OH. Therefore, changes to O₃ concentrations lead to a response in CH₄ and, as a consequence, a response in peroxy radical con-

Potential climate forcing of land use and land cover change

D. S. Ward et al.

Title Page

Abstract

Introduction

Conclusions

References

Tables

Figures

⏪

⏩

◀

▶

Back

Close

Full Screen / Esc

Printer-friendly Version

Interactive Discussion



centrations (Naik et al., 2005). The changes in peroxy radical concentrations, an end result of the changes in emissions of O_3 precursors caused by LULCC or other anthropogenic activities, feeds back onto O_3 , a response which is approximated with the following expression (Naik et al., 2005):

$$5 \quad (\Delta O_3)_{\text{primary}} = \frac{\Delta[\text{CH}_4]}{[\text{CH}_4]} \cdot 6.4 \text{ DU} \quad (10)$$

We use a value of $0.032 \pm 0.006 \text{ W m}^{-2} \text{ DU}^{-1}$ (Forster et al., 2007) to compute the additional RF of O_3 caused by this process, known as the primary mode response.

3.4.2 CO_2 , CH_4 , N_2O

10 After changes in the long-lived greenhouse gas concentrations due to LULCC or other anthropogenic emissions are calculated, simple expressions from the IPCC TAR (Ramaswamy et al., 2001) can be used to estimate the adjusted radiative forcing (ΔF). For CO_2 :

$$15 \quad \Delta F = 5.35 \cdot \ln \left(\frac{C}{C_0} \right) \quad (11)$$

Here C_0 is the atmospheric CO_2 concentration in the unperturbed state (with no LULCC emissions, or no emissions from other anthropogenic activities) and C is the perturbed atmospheric CO_2 concentration containing both all anthropogenic contributions. In this way the CO_2 saturation effect of the different perturbed CO_2 concentrations on the RF is taken into account.

Potential climate forcing of land use and land cover change

D. S. Ward et al.

Title Page

Abstract

Introduction

Conclusions

References

Tables

Figures

⏪

⏩

◀

▶

Back

Close

Full Screen / Esc

Printer-friendly Version

Interactive Discussion



Likewise, the adjusted RF for the changes in CH₄ and N₂O concentrations can be computed with the following expressions (Ramaswamy et al., 2001):

$$\Delta F = 0.036 \left(\sqrt{M} - \sqrt{M_0} \right) - [f(M, N_0) - f(M_0, N_0)] \quad (12)$$

$$\Delta F = 0.12 \left(\sqrt{N} - \sqrt{N_0} \right) - [f(M_0, N) - f(M_0, N_0)] \quad (13)$$

$$f(M, N) = 0.47 \cdot \ln[1 + 2.01 \times 10^{-5} (M \cdot N)^{0.75} + 5.31 \times 10^{-15} M (M \cdot N)^{1.52}] \quad (14)$$

using the average tropospheric concentrations of CH₄ (ppb) and N₂O (ppb) in the perturbed state with LULCC or other anthropogenic emissions removed (M and N , respectively), and in the unperturbed, reference state (M_0 and N_0 , respectively). Equation (12) corresponds to CH₄ and Eq. (13) corresponds to N₂O.

3.4.3 Aerosol effects

Aerosols impact radiative transfer directly by scattering and absorbing shortwave and some longwave radiation, and also indirectly by their effects on clouds. We compute the direct effect of changes in aerosols from LULCC by running the CAM5 radiation online in a diagnostic mode separately from the prognostic radiation in the model. The radiation package is run at every timestep through the model atmosphere with all aerosols and again with aerosols removed from interactions with radiation. The difference in top-of-atmosphere net radiative flux when aerosols are removed is the all-sky direct radiative effect. We compute this effect for shortwave and longwave interactions.

Indirect effects are defined here as the change in total cloud forcing between the simulations with and without LULCC (referenced to 1850), where total cloud forcing is the sum of the longwave and shortwave cloud forcing. This quantity is assessed after the direct effects of aerosols have been removed with the online diagnostics. Therefore, the sum of the direct effects and indirect effects of aerosols is equal to the total radiative change caused by aerosols in the CAM5 simulations.

Potential climate forcing of land use and land cover change

D. S. Ward et al.

Title Page

Abstract

Introduction

Conclusions

References

Tables

Figures

⏪

⏩

◀

▶

Back

Close

Full Screen / Esc

Printer-friendly Version

Interactive Discussion



Potential climate forcing of land use and land cover change

D. S. Ward et al.

Title Page

Abstract

Introduction

Conclusions

References

Tables

Figures

⏪

⏩

◀

▶

Back

Close

Full Screen / Esc

Printer-friendly Version

Interactive Discussion

In CAM5, the indirect effects of aerosols on clouds includes the first indirect effect by which aerosols, acting as cloud condensation nuclei, lead to changes in cloud droplet size and, as a consequence, cloud albedo. CAM5 also simulates aerosol/cloud interactions that are considered secondary indirect effects. These include aerosol impacts on stratiform cloud lifetime and height, and the semi-direct effect. The semi-direct effect refers to the change in cloud fraction that results from the warming of an air layer by aerosol absorption of shortwave radiation (Lohmann and Feichter, 2005). Aerosol impacts on convective clouds are not included in our simulations.

These aspects of the CAM5 microphysics may lead to bias in our RF calculations when compared to the model consensus RFs from the IPCC AR4 (Forster et al., 2007). The IPCC central estimate for the indirect aerosol effect includes only the first indirect effect (aerosol impact on cloud albedo though changes in cloud droplet size). For this reason, and because models generally disagree on the magnitude of the aerosol effects (Forster et al., 2007), we use the IPCC AR4 central estimate aerosol direct and indirect effects for calculating the year 2010 RF and use our model results to determine the proportion of the total anthropogenic aerosols effects due to LULCC. Using the RFs from the IPCC AR4 results in a $\sim 25\%$ decrease in the year 2010 LULCC aerosol direct and indirect RF magnitudes compared to our model. We apply the same scaling to the aerosol effects in all future scenarios. Central estimates of the aerosol effective RF, both direct and indirect, from the IPCC AR5 report total -0.9 W m^{-2} (Myhre et al., 2013). Our calculations of LULCC RFs would be nearly unchanged if we used the AR5 values for aerosol forcings, but we estimate that the proportion of total anthropogenic RF from LULCC would be decreased by roughly 5%.

In addition to these effects in the atmosphere, light-absorbing aerosols, particularly BC and dust, can decrease the albedo of the Earth's surface when they are deposited onto snow and ice surfaces. The Snow, Ice, and Aerosol Radiative (SNICAR) model (Flanner and Zender, 2006) is run online with CAM5 to simulate this process and estimate the RF. For all cases the RF of aerosol deposition onto snow and ice surfaces is between 0 and 0.03 W m^{-2} . Note that we only capture aerosol deposition on snow and

ice covering land and not over sea. This will reduce our estimates of the RF compared to estimates including sea-ice, although the RF from aerosol deposition onto sea-ice is thought to be less important than deposition onto land-covering snow and ice (Flanner et al., 2007).

5 3.4.4 Land surface albedo

LULCC activities change vegetation cover and type, affect forest canopy coverage, and alter wildfire activity, all of which impact land surface albedo. The albedo changes, apart from those caused by fires, are simulated by CLM. Monthly averages for solar radiation incident upon the surface (after accounting for attenuation by monthly average cloud cover) are multiplied by the surface albedo with LULCC and without LULCC for each model grid point. The RF equals the global annual average difference between the outgoing solar radiation with LULCC and without LULCC. The impact of the albedo changes may be further moderated by changes in cloudiness (Lawrence and Chase, 2010), which we did not consider in this analysis.

15 For albedo changes from wildfire activity, post-fire albedo response curves (Ward et al., 2012) are applied to the difference in burned area with LULCC and without LULCC at each grid point. Fires lead to negative (cooling) RF from albedo changes on a global average (Ward et al., 2012). Since historical and projected LULCC reduced burned area in CLM, the result was a small but positive RF in all cases, acting in the
20 opposite direction of the overall negative LULCC albedo change RF.

3.4.5 Aerosol biogeochemical feedbacks

The importance of aerosol biogeochemical feedbacks onto CO₂ concentrations is beginning to be recognized and known impacts have recently been quantified (Mahowald, 2011). We consider changes to terrestrial uptake of carbon by the addition of nutrients
25 (N, phosphorous (P), and iron (Fe)) transported by aerosols, and also by modifications of climate.

Potential climate forcing of land use and land cover change

D. S. Ward et al.

Title Page

Abstract

Introduction

Conclusions

References

Tables

Figures

⏪

⏩

◀

▶

Back

Close

Full Screen / Esc

Printer-friendly Version

Interactive Discussion



Potential climate forcing of land use and land cover change

D. S. Ward et al.

Title Page

Abstract

Introduction

Conclusions

References

Tables

Figures

⏪

⏩

◀

▶

Back

Close

Full Screen / Esc

Printer-friendly Version

Interactive Discussion

N deposition from anthropogenic sources fertilizes vegetation growth and increases the drawdown of CO_2 , causing a present day RF of -0.12 to -0.35 W m^{-2} . We multiply this forcing by the ratio of N emissions (NH_3 , NO_x) from LULCC or other anthropogenic activities for each case to year 2010 total anthropogenic N emissions.

Fertilization can also be enhanced by deposition of P and Fe from fire emissions. Changes in Amazonian fire activity have led to an estimated -0.12 to 0 W m^{-2} RF from increased CO_2 drawdown due to fertilization by P. Deposition of fire-emitted Fe to the oceans could be responsible for a RF of $-0.02 \pm 0.02 \text{ W m}^{-2}$ (Ward et al., 2012). We scaled these RFs by the changes in fire activity due to LULCC in the Amazon (for P) and globally (for Fe) for all cases. These result in small RFs (less than $\pm 0.05 \text{ W m}^{-2}$) such that N dominates these biogeochemical feedbacks.

Finally, changes in global surface temperature caused by the previously described RFs of LULCC and non-LULCC activities lead to a response in carbon uptake by the terrestrial biosphere and the ocean (Mahowald, 2011). Moreover, aerosols affect vegetation by redistributing precipitation and changing the ratio of diffuse to direct radiation incident on the surface. While not very well understood, these biogeochemical feedbacks can be estimated by coupled carbon-climate models that suggest a roughly linear response of between 0 and 40 ppm CO_2 for a RF of 1.4 W m^{-2} (Mahowald et al., 2011). We sum the total RF of LULCC for all cases from greenhouse gases, aerosol effects and albedo changes, to estimate the impact of the potential changes in climate on atmospheric CO_2 . In all cases, since the total RF from LULCC is positive, the RF of the feedback onto CO_2 concentrations is also positive.

The total RFs of these biogeochemical feedbacks are included with the CO_2 RF in the tables and figures since they impact climate through changing CO_2 concentrations.

3.5 Uncertainty

The uncertainty in these RF estimates arises largely from the uncertainty in modeling the effects of aerosols and modeling the impacts of climate, CO_2 changes, and LULCC on the carbon cycle. Our model predicts less uptake of anthropogenic carbon in natural

troposphere, and as a result, a 20 % reduction in CH₄ lifetime with respect to removal by reaction with OH (Sect. 3.3.2).

From CAM4 simulations of atmospheric chemistry we find that tropospheric O₃ increases from 192 Tg in 1850 to 304 Tg in 2010, when all anthropogenic activities are included. The O₃ increase of 112 Tg falls within the range of previous estimates (Lamarque et al., 2005). Here we separate the increase in O₃ concentrations into a non-LULCC contribution, 87 %, and a LULCC contribution, 13 % (Sect. 3.4.1). The large non-LULCC contribution is attributable to additional O₃ formation from NO_x emissions from fossil fuel burning sources. The contribution of LULCC to O₃ change results from the combination of several competing effects (Ganzeveld et al., 2010) including changes in the production of secondary organic aerosol from biogenic precursor gases (virtually unchanged by historical LULCC on a global average) and decreases in emissions from wildfires (Table 2). The increase in tropospheric O₃ from LULCC is partially compensated for by a slight increase in the dry deposition of O₃ with LULCC (6 %) between 1850 and 2010 as a result of the LULCC-enhanced O₃ concentration and despite the decrease in O₃ removal efficiency in deforested areas, similar to the findings of Ganzeveld et al. (2010). The small contribution of LULCC to global “short-lived” O₃ concentrations is augmented by additional O₃ (2.5 DU in 2010) produced in response to long-term increases in CH₄ (primary mode response; Sect. 3.4.1). The additional O₃ from this response accounts for 60 % of the LULCC O₃ RF of 0.12 W m⁻² in 2010. The primary mode response O₃ is less important for non-LULCC activities because of the smaller CH₄ contribution from these activities.

We assume that long-lived greenhouse gases, CO₂, CH₄, and N₂O, with lifetimes on the order of years to centuries, are sufficiently well-mixed in the atmosphere that the forcing from these gases is spatially homogeneous (Table 5). The lifetime of tropospheric O₃ is considerably shorter, on the order of weeks, meaning concentrations can vary spatially, becoming higher near areas of O₃ production and remaining below the global average in remote regions away from areas of O₃ production. The RF varies

Potential climate forcing of land use and land cover change

D. S. Ward et al.

Title Page

Abstract

Introduction

Conclusions

References

Tables

Figures

⏪

⏩

◀

▶

Back

Close

Full Screen / Esc

Printer-friendly Version

Interactive Discussion

Potential climate forcing of land use and land cover change

D. S. Ward et al.

Title Page

Abstract

Introduction

Conclusions

References

Tables

Figures

⏪

⏩

◀

▶

Back

Close

Full Screen / Esc

Printer-friendly Version

Interactive Discussion

in space with the concentration, although, these heterogeneities are moderate for O_3 . The RF at 80 % of grid points is within $\pm 0.07 \text{ W m}^{-2}$ of the global mean RF (Table 5).

While the positive RF from non-LULCC greenhouse gas emissions is offset to some extent by concurrent emissions of aerosols, LULCC causes both increases and decreases in aerosol emissions resulting in nearly neutral aerosol RFs for the present day (Fig. 5). The contrasting changes in aerosol sources from LULCC are evident by the spatial variability in AOD caused by historical LULCC, ranging between -0.18 to 0.29 (Table 5). Global average aerosol optical depth (AOD) is increased by LULCC in 2010 and in 2100 for the RCP4.5, RCP6.0 and worst case scenario scenarios, and decreased by RCP2.6 and RCP8.5 LULCC, but in all cases the change is less than 0.01. The RF from aerosol deposition onto snow and ice surfaces is negligible on a global average (0.01 W m^{-2} for historical LULCC) but exceeds $\pm 1 \text{ W m}^{-2}$ in some locations (Table 5). We also consider the impacts of aerosols and trace gas species on atmospheric CO_2 due to bio-fertilization by deposition of P, Fe and N emitted from fires, and N from agriculture (NH_3 , NO_x , N_2O). For present day emissions of these species from LULCC activities (and land cover change impacts on fires), the drawdown of CO_2 , enhanced particularly by agricultural emissions of N, leads to a negative RF of -0.10 W m^{-2} that nearly compensates for the positive RF from the greenhouse effect of agricultural N_2O emissions (0.14 W m^{-2}), a noteworthy aspect of agricultural emissions that was also suggested by Zaehle et al. (2011).

Estimates for the global RF from albedo changes range from -0.10 (Skeie et al., 2011) to -0.28 W m^{-2} (Lawrence et al., 2012), with a substantial percentage, potentially 25 %, caused by preindustrial LULCC (Pongratz et al., 2009). Further estimates (Betts, 2001; Betts et al., 2007; Davin et al., 2007) fall near the IPCC AR4 central estimate of -0.2 W m^{-2} (Forster et al., 2007). The RF from albedo changes is near zero in most locations but has a high magnitude, up to 5 W m^{-2} , in some localities on an annual average (Table 5), similar to the findings of Betts et al. (2007). Our estimate for the global RF from historical land surface albedo change, -0.05 W m^{-2} , is at the higher end of the range of previously published estimates, yet still within the 90 % con-

Potential climate forcing of land use and land cover change

D. S. Ward et al.

Title Page

Abstract

Introduction

Conclusions

References

Tables

Figures

⏪

⏩

◀

▶

Back

Close

Full Screen / Esc

Printer-friendly Version

Interactive Discussion

the worst case scenario to place an upper bound on the potential LULCC RF for this century. The worst case scenario, in which all arable land is converted to agricultural land and all remaining land that is pasturable is converted to grasses by the year 2100, does not take some important agricultural factors, such as changes in crop yields and per capita caloric intake, into account, but was created as a plausible limit to cropland expansion on Earth. Since we designate arable land using a measure of climate suitability (Sect. 2), following Ramankutty et al. (2002), crop area could conceivably expand beyond this limit with the use of irrigation. In fact, areas of South Asia currently support more agriculture than estimates of climate suitability suggest they should (Ramankutty et al., 2002).

In the worst case scenario, crop area roughly doubles by the year 2050, and continues to increase at the same rate to 2100. The rate of deforestation required to accommodate the expanded agriculture is three times greater than upper estimates from the RCPs for year 2000–2030 forest loss (Fig. 7), resulting in the near complete removal of tropical forests by the year 2100 (Fig. 4), and a global release of ~ 500 PgC from vegetation to the atmosphere. Loss of soil C often accompanies forest conversion to crops or grasses (Lal, 2004) but this process is not well simulated in this generation of terrestrial models. House et al. (2002) estimate terrestrial C loss from a complete deforestation to be between 450 to 820 PgC, with much of the uncertainty in the range due to different estimates of C loss from soils. Our CLM3 experiment resulted in negligible soil C change globally, even after applying the drastic forest and crop area changes of the worst case scenario. Still, loss of C from vegetation alone in the worst case scenario corresponds to roughly two-thirds of the value of the proven reserves of fossil fuels (760 PgC) (Meinshausen et al., 2009). The substantial loss of terrestrial C to the atmosphere in the worst case scenario leads to a RF of 1.6 W m^{-2} for CO_2 (Fig. 6). The magnitudes of all other forcing agents are enhanced in this scenario, leading to a sum RF of $4.3 \pm 1.0 \text{ W m}^{-2}$ at the year 2100.

4.3 Total radiative forcing compared with CO₂-derived radiative forcing

On average over all converted land types and land management histories, CO₂ RF from LULCC is enhanced by the accompanying (although not necessarily concurrent) emissions of non-CO₂ greenhouse gases and aerosols, such that the total RF is 2 to 3 times that of the CO₂ alone. For example, we estimate the direct carbon release from LULCC between 1850–2010 to be 140 PgC, leading to a RF from CO₂ of $\sim 0.4 \text{ W m}^{-2}$ in 2010, or about half of the total LULCC RF. In contrast, for other anthropogenic activities the RF from CO₂ and the total RF are roughly equal (Figs. 5 and 6). Therefore, while LULCC accounted for about 20 % of anthropogenic CO₂-equivalent emissions in 2010 (Tubiello et al., 2013), its contribution to the anthropogenic RF is 45 % (+30 %, –20 %). We can express this enhancement factor as the ratio of the sum RF to the CO₂ RF for LULCC, divided by the same ratio for other anthropogenic activities (FF+), or $E = (\text{RF}_{\text{sum}}/\text{RF}_{\text{CO}_2})_{\text{LULCC}}/(\text{RF}_{\text{sum}}/\text{RF}_{\text{CO}_2})_{\text{FF+}}$. For all future LULCC scenarios the enhancement factor is between 2.1 to 3.1 (Table 6). We compute the maximum enhancement of the CO₂ RF for the RCP4.5 scenario ($E = 3.1$). In the development of the RCP4.5 scenario, international carbon trading incentivizes preservation of forests and reforestation, which reduces CO₂ emissions and the resulting CO₂ RF from LULCC, increasing the enhancement factor.

5 Conclusions

Effective strategies for mitigation of human impacts on global climate require an understanding of the major sources of those impacts (Unger et al., 2010). Anthropogenic land use and changes to land cover have long been recognized as important contributors to global climate forcing (Feddema et al., 2005), and yet most studies on this topic focus on either land use (e.g. Unger et al., 2010) or land cover change (e.g. Davin et al., 2007; Pongratz et al., 2009), but not both. In this study we compute the fraction of

Potential climate forcing of land use and land cover change

D. S. Ward et al.

Title Page

Abstract

Introduction

Conclusions

References

Tables

Figures



Back

Close

Full Screen / Esc

Printer-friendly Version

Interactive Discussion

anthropogenic RF that results from LULCC activities including a more comprehensive range of forcing agents.

Current estimates of the LULCC C flux between 1850 and 2000 are between 108 PgC and 188 PgC (Houghton, 2010), while here we estimate 131 PgC. Estimates from this study using the future scenarios analyzed in the IPCC (the representative concentration scenarios or RCPs) suggest between 20 and 210 C will be released, consistent with Strassmann et al. (2008), and at the higher end of the model range reported by Brovkin et al. (2013). Our model underpredicts the uptake of land carbon relative to other models (e.g Arora et al., 2013), and unlike other estimates includes the explicit interplay between changes in land use and fires (e.g. Marlon et al., 2008; Kloster et al., 2010). The RCP scenarios were designed to cover a diverse set of pathways and create a broad range in possible outcomes for the next century (Moss et al., 2010). Given that the RCP scenarios all project decreases in global forest area loss rates in the 21st century relative to current rates, these scenarios are likely to be lower bounds on deforestation rates in the future (Fig. 7). To explore higher rates of global forest loss and crop and pasture expansions, we introduce a worst case scenario, in which all the land which is likely to be arable is converted to agriculture and pasture usage by 2100. Since the rates of deforestation in this scenario are higher than current rates, this scenario is an upper bound on what could occur. We calculate that with the intense pressures on land inherent to this scenario, between 590 and 700 PgC would be released from LULCC in this century.

We find that the total RF from LULCC is 2 to 3 times the RF from CO₂ alone when additional positive forcings from non-CO₂ greenhouse gases and relatively small forcings from aerosols and surface albedo are considered. The RF of other anthropogenic activities (largely fossil fuels) in 2010 and in 2100 (RCP4.5), relative to 1850, includes a large magnitude negative aerosol forcing that offsets enough of the warming contribution from greenhouse gases that the total RF matches closely with the RF from CO₂. The result of this enhancement of the LULCC RF with respect to its CO₂ emissions, and lack of enhancement of the other anthropogenic activities RF, is a 45 % LULCC

Potential climate forcing of land use and land cover change

D. S. Ward et al.

Title Page

Abstract

Introduction

Conclusions

References

Tables

Figures



Back

Close

Full Screen / Esc

Printer-friendly Version

Interactive Discussion



et al., 2011), our study substantiates that not only energy usage but land use and land cover change needs to remain a focus of climate change mitigation.

Appendix A

Computing uncertainties

5 The uncertainties in RF estimations are substantial (Forster et al., 2007) and include uncertainties in the model representation of physical and chemical processes, model internal variability and imperfect knowledge of processes. Here we describe the calculation of uncertainties for the RFs reported in this paper and we assume the uncertainty has three sources: model and RF computations, partitioning of emissions
10 between LULCC and non-LULCC, and uncertainty in the emissions from future fires (values given in Table A1).

A1 Anthropogenic RF calculation uncertainties

For the uncertainty in the total anthropogenic RF calculations, we take the 90 % confidence intervals generated by the IPCC (Forster et al., 2007) for each forcing agent and assume these represent a Gaussian probability density function around the central
15 estimate (Table A1, “Model” column). This assumption may not be appropriate for all forcing agents if the goal were to compute uncertainties that could be interpreted probabilistically. Therefore we stress that the calculated uncertainties are rough estimates and should not be interpreted as probabilistic. We propagate this uncertainty to LULCC and non-LULCC by multiplying by the corresponding fraction of the RF from LULCC or non-LULCC, or in the case of the aerosol forcings, by the fraction of AOD from LULCC
20 or non-LULCC. Since we use the IPCC aerosol forcings in our total LULCC RF estimates, we do not include uncertainty introduced by the secondary aerosol effects.

Potential climate forcing of land use and land cover change

D. S. Ward et al.

Title Page

Abstract

Introduction

Conclusions

References

Tables

Figures

⏪

⏩

◀

▶

Back

Close

Full Screen / Esc

Printer-friendly Version

Interactive Discussion



A2 Partitioning uncertainty

The partitioning uncertainty is determined from previous estimates of the error in sector-specific trace gas and aerosol emissions. We define this uncertainty as the maximum range in the ratio of LULCC to non-LULCC emissions that could result from the two sources varying from plus to minus one standard deviation of their own source-specific uncertainty (Table A1, “Partitioning” column).

The source uncertainties for trace gases CO₂, CH₄, NH₃, NO_x, and N₂O are taken from the IPCC AR4 (Forster et al., 2007). The source uncertainties in emissions of N species (that is, the range in the ratio of LULCC N emissions to non-LULCC N emissions varying within the uncertainties from each source reported by Forster et al., 2007) are combined to produce the partitioning uncertainty of the aerosol biogeochemical feedback onto CO₂ concentrations. The feedback of RF from non-LULCC and LULCC separately onto the carbon cycle (Sect. 3.3.3) is also included here as part of the CO₂ partitioning uncertainty. The partitioning uncertainty for CH₄ is combined with uncertainty in global sinks of CH₄ (from Forster et al., 2007) that affect our understanding of the CH₄ atmospheric lifetime. For emissions of CO (used in O₃ partitioning uncertainty) we estimate a two times uncertainty in all emissions (Unger et al., 2010). Similarly, we begin with a two times uncertainty in aerosol emissions, as this has been estimated for carbonaceous aerosols (Unger et al., 2010), but noting that the emissions of dust and SOA are more uncertain than emissions of carbonaceous aerosols, we double this uncertainty for aerosol emissions (4 times uncertainty). The partitioning uncertainties for halocarbon emissions and land surface albedo changes are zero since we only consider one source, LULCC or non-LULCC, for these forcing agents.

A3 Summing the uncertainties

Using the Monte Carlo method with $N = 100000$ iterations, and assuming that the different forcing agents vary independently of one another, we produce Gaussian probability density functions for the combined RF (all agents, and LULCC and other an-

Potential climate forcing of land use and land cover change

D. S. Ward et al.

Title Page

Abstract

Introduction

Conclusions

References

Tables

Figures

⏪

⏩

◀

▶

Back

Close

Full Screen / Esc

Printer-friendly Version

Interactive Discussion



Potential climate forcing of land use and land cover change

D. S. Ward et al.

Title Page

Abstract

Introduction

Conclusions

References

Tables

Figures

◀

▶

◀

▶

Back

Close

Full Screen / Esc

Printer-friendly Version

Interactive Discussion

thropogenic sources) and for the LULCC RF (all agents, only LULCC sources). Adding these uncertainties together (root of the sum of squares) gives the uncertainty in the fraction of anthropogenic RF attributable to LULCC (Table 3). The assumption of independence among forcing agents is not perfect. For example, NO_x concentrations are used to predict changes in O₃, CH₄, and total N, and the same aerosol emissions are used to estimate several different forcings. However, given that there are large uncertainties specific to the calculation of each forcing agent, and apart from those associated with emissions, we retain the assumption of independence for approximating the sum of the uncertainties.

We apply the same uncertainties to the future RFs for LULCC and add additional uncertainty due to variability in global fire activity between 2010–2100 that is due to the different atmospheric forcing used in these simulations. We define this uncertainty as the total range in RF caused by using the different atmospheric forcing datasets to drive global fires in CLM (Table A1, “Fire” columns). The different forcing datasets were chosen to represent a large spread in projected temperature and precipitation by the year 2100 (Kloster et al., 2012). The uncertainties of the different forcing agents with regard to fire emissions are not independent of each other and, therefore, are added directly to the sum uncertainties after the Monte Carlo simulations have determined the sum of the other, more independent, uncertainties.

Acknowledgements. We would like to acknowledge the feedback and assistance of Jasper Kok, Maria val Martin, Jim Randerson, Wendy Woolford, and Jiao Lan. We recognize funding from the National Science Foundation (NSF AGS-0758369, NSF-EaSM1049033, NSF-CI0832782) and Guggenheim Foundation. Model integrations were performed with a National Center for Atmospheric Research facility, which is sponsored by the NSF.

References

- Albani, S., Mahowald, N. M., Perry, A. T., Scanza, R. A., Zender, C. S., Heavens, N. G., Maggi, V., Kok, J. F., and Otto-Bliesner, B. L.: Improved dust representation in the Community Atmosphere Model, *Journal of Advances in Modeling Earth Systems*, in review, 2014.
- 5 Allen, M. R., Frame, D. J., Huntingford, C., Jones, C. D., Lowe, J. A., Meinshausen, M., and Meinshausen, N.: Warming caused by cumulative carbon emissions towards the trillionth tonne, *Nature*, 458, 1163–1166, 2009.
- Arora, V. K. and Boer, G. J.: Uncertainties in the 20th century carbon budget associated with land use change, *Glob. Change Biol.*, 16, 3327–3348, doi:10.1111/j.1365-2486.2010.02202.x, 2010.
- 10 Arora, V. K., Boer, G. J., Friedlingstein, P., Eby, M., Jones, C. D., Christian, J. R., Bonan, G., Bopp, L., Brovkin, V., Cadule, P., Hajima, T., Ilyina, T., Lindsay, K., Tjiputra, J. F., and Wu, T.: Carbon-concentration and carbon-climate feedbacks in CMIP5 Earth System Models, *J. Climate*, 26, 5289–5314, doi:10.1175/jcli-d-12-00494.1, 2013.
- 15 Ashworth, K., Wild, O., and Hewitt, C. N.: Sensitivity of isoprene emissions estimated using MEGAN to the time resolution of input climate data, *Atmos. Chem. Phys.*, 10, 1193–1201, doi:10.5194/acp-10-1193-2010, 2010.
- Avila, F. B., Pitman, A. J., Donat, M. G., Alexander, L. V., and Abramowitz, G.: Climate model simulated changes in temperature extremes due to land cover change, *J. Geophys. Res.*, 117, D04108, doi:10.1029/2011jd016382, 2012.
- 20 Bala, G., Caldeira, K., Wickett, M., Phillips, T. J., Lobell, D. B., Delire, C., and Mirin, A.: Combined climate and carbon-cycle effects of large-scale deforestation, *P. Natl. Acad. Sci. USA*, 104, 6550–6555, doi:10.1073/pnas.0608998104, 2007.
- Batjes, N.: ISRIC-WISE Global Data Set of Derived Soil Properties on a 0.5 by 0.5 Degree Grid (Version 3.0), ISRIC-World Soil Inf. Rep., 8, the Netherlands, 2005.
- 25 Betts, R. A.: Biogeophysical impacts of land use on present-day climate: near-surface temperature change and radiative forcing, *Atmos. Sci. Lett.*, 2, 39–51, 2001.
- Betts, R. A.: Comparing apples with oranges, *Nature Reports Climate Change*, 2, 7–8, doi:10.1038/climate.2007.74, 2008.
- 30 Betts, R. A., Falloon, P. D., Goldewijk, K. K., and Ramankutty, N.: Biogeophysical effects of land use on climate: model simulations of radiative forcing and large-scale temperature change, *Agr. Forest Meteorol.*, 142, 216–233, doi:10.1016/j.agrformet.2006.08.021, 2007.

Potential climate forcing of land use and land cover change

D. S. Ward et al.

Title Page

Abstract

Introduction

Conclusions

References

Tables

Figures

⏪

⏩

◀

▶

Back

Close

Full Screen / Esc

Printer-friendly Version

Interactive Discussion



Potential climate forcing of land use and land cover change

D. S. Ward et al.

Title Page

Abstract

Introduction

Conclusions

References

Tables

Figures

⏪

⏩

◀

▶

Back

Close

Full Screen / Esc

Printer-friendly Version

Interactive Discussion

- Brovkin, V., Ganopolski, A., Claussen, M., Kubatzki, C., and Petoukhov, V.: Modelling climate response to historical land cover change, *Global Ecol. Biogeogr.*, 8, 509–517, doi:10.1046/j.1365-2699.1999.00169.x, 1999.
- Brovkin, V., Sitch, S., von Bloh, W., Claussen, M., Bauer, E., and Cramer, W.: Role of land cover changes for atmospheric CO₂ increase and climate change during the last 150 years, *Glob. Change Biol.*, 10, 1253–1266, doi:10.1111/j.1365-2486.2004.00812.x, 2004.
- Brovkin, V., Claussen, M., Driesschaert, E., Fichefet, T., Kicklighter, D., Loutre, M. F., Matthews, H. D., Ramankutty, N., Schaeffer, M., and Sokolov, A.: Biogeophysical effects of historical land cover changes simulated by six Earth system models of intermediate complexity, *Clim. Dynam.*, 26, 587–600, doi:10.1007/s00382-005-0092-6, 2006.
- Brovkin, V., Boysen, L., Arora, V. K., Boisier, J. P., Cadule, P., Chini, L., Claussen, M., Friedlingstein, P., Gayler, V., van den Hurk, B. J. J. M., Hurtt, G. C., Jones, C. D., Kato, E., de Noblet-Ducoudré, N., Pacifico, F., Pongratz, J., and Weiss, M.: Effect of anthropogenic land-use and land-cover changes on climate and land carbon storage in CMIP5 projections for the twenty-first century, *J. Climate*, 26, 6859–6881, doi:10.1175/jcli-d-12-00623.1, 2013.
- Cherubini, F., Bright, R. M., and Strømman, A. H.: Site-specific global warming potentials of biogenic CO₂ for bioenergy: contributions from carbon fluxes and albedo dynamics, *Environ. Res. Lett.*, 7, 045902, doi:10.1088/1748-9326/7/4/045902, 2012.
- Ciais, P., Sabine, C., Bala, G., Bopp, L., Brovkin, V., Canadell, J. G., Chhabra, A., Defries, R., Galloway, J., Heimann, M., Jones, C., Le Quere, C., Myneni, R. B., Piao, S., and Thornton, P.: Carbon and other biogeochemical cycles, in: *Climate Change 2013: The Physical Science Basis, Contribution of Working Group I to the Fifth Assessment Report of the Intergovernmental Panel on Climate Change*, edited by: Stocker, T. F., Qin, D., Plattner, G.-K., Tignor, M., Allen, S. K., Boschung, J., Nauels, A., Xia, Y., Bex, V., and Midgley, P. M., Cambridge University Press, New York, NY, USA, 465–570, 2013.
- Claussen, M., Brovkin, V., and Ganopolski, A.: Biogeophysical versus biogeochemical feedbacks of large-scale land cover change, *Geophys. Res. Lett.*, 28, 1011–1014, doi:10.1029/2000gl012471, 2001.
- Conley, A. J., Lamarque, J.-F., Vitt, F., Collins, W. D., and Kiehl, J.: PORT, a CESM tool for the diagnosis of radiative forcing, *Geosci. Model Dev.*, 6, 469–476, doi:10.5194/gmd-6-469-2013, 2013.

Potential climate forcing of land use and land cover change

D. S. Ward et al.

Title Page

Abstract

Introduction

Conclusions

References

Tables

Figures

◀

▶

◀

▶

Back

Close

Full Screen / Esc

Printer-friendly Version

Interactive Discussion

Davin, E. L., de Noblet-Ducoudré, N., and Friedlingstein, P.: Impact of land cover change on surface climate: relevance of the radiative forcing concept, *Geophys. Res. Lett.*, 34, L13702, doi:10.1029/2007gl029678, 2007.

Defries, R. S., Bounoua, L., and Collatz, G. J.: Human modification of the landscape and surface climate in the next fifty years, *Glob. Change Biol.*, 8, 438–458, doi:10.1046/j.1365-2486.2002.00483.x, 2002.

Emmons, L. K., Walters, S., Hess, P. G., Lamarque, J.-F., Pfister, G. G., Fillmore, D., Granier, C., Guenther, A., Kinnison, D., Laepple, T., Orlando, J., Tie, X., Tyndall, G., Wiedinmyer, C., Baughcum, S. L., and Kloster, S.: Description and evaluation of the Model for Ozone and Related chemical Tracers, version 4 (MOZART-4), *Geosci. Model Dev.*, 3, 43–67, doi:10.5194/gmd-3-43-2010, 2010.

Enting, I. G., Wigley, T., Heimann, M., and Scientific, C.: Future Emissions and Concentrations of Carbon Dioxide: Key Ocean/Atmosphere/Land Analyses, 31, CSIRO Australia, Australia, 1994.

FAO: Global Forest Resources Assessment 2010, Rome, 2010.

Feddema, J. J., Oleson, K. W., Bonan, G. B., Mearns, L. O., Buja, L. E., Meehl, G. A., and Washington, W. M.: The importance of land-cover change in simulating future climates, *Science*, 310, 1674–1678, doi:10.1126/science.1118160, 2005.

Flanner, M. G. and Zender, C. S.: Linking snowpack microphysics and albedo evolution, *J. Geophys. Res.-Atmos.*, 111, D12208, doi:10.1029/2005JD006834, 2006.

Flanner, M. G., Zender, C. S., Randerson, J. T., and Rasch, P. J.: Present-day climate forcing and response from black carbon in snow, *J. Geophys. Res.-Atmos.*, 112, D11202, doi:10.1029/2006JD008003, 2007.

Foley, J. A., Defries, R., Asner, G. P., Barford, C., Bonan, G., Carpenter, S. R., Chapin, F. S., Coe, M. T., Daily, G. C., Gibbs, H. K., Helkowski, J. H., Holloway, T., Howard, E. A., Kucharik, C. J., Monfreda, C., Patz, J. A., Prentice, I. C., Ramankutty, N., and Snyder, P. K.: Global consequences of land use, *Science*, 309, 570–574, doi:10.1126/science.1111772, 2005.

Foley, J. A., Ramankutty, N., Brauman, K. A., Cassidy, E. S., Gerber, J. S., Johnston, M., Mueller, N. D., O'Connell, C., Ray, D. K., West, P. C., Balzer, C., Bennett, E. M., Carpenter, S. R., Hill, J., Monfreda, C., Polasky, S., Rockstrom, J., Sheehan, J., Siebert, S., Tilman, D., and Zaks, D. P. M.: Solutions for a cultivated planet, *Nature*, 478, 337–342, 2011.

Potential climate forcing of land use and land cover change

D. S. Ward et al.

Title Page

Abstract

Introduction

Conclusions

References

Tables

Figures

⏪

⏩

◀

▶

Back

Close

Full Screen / Esc

Printer-friendly Version

Interactive Discussion

- Forster, P., Ramaswamy, V., Artaxo, P., Bernsten, T., Betts, R., Fahey, D. W., Haywood, J., Lean, J., Lowe, D. C., Myhre, G., Nganga, J., Prinn, R., Raga, G., Schulz, M., and Dorland, R. V.: Changes in atmospheric constituents and in radiative forcing, in: *Climate Change 2007: The Physical Science Basis, Contribution of Working Group I to the Fourth Assessment Report of the Intergovernmental Panel on Climate Change*, edited by: Solomon, S., Qin, D., Manning, M., Chen, Z., Marquis, M., Averyt, K. B., Tignor, M., and Miller, H. L., Cambridge University Press, New York City, NY, USA, 129–234, 2007.
- Friedlingstein, P., Meinshausen, M., Arora, V. K., Jones, C. D., Anav, A., Liddicoat, S. K., and Knutti, R.: Uncertainties in CMIP5 climate projections due to carbon cycle feedbacks, *J. Climate*, 27, 511–526, doi:10.1175/JCLI-D-12-00579.1, 2013.
- Fujino, J., Nair, R., Kainuma, M., Masui, T., and Matsuoka, Y.: Multi-gas mitigation analysis on stabilization scenarios using aim global model, *Energ. J.*, 27, 343–353, 2006.
- Ganzeveld, L., Bouwman, L., Stehfest, E., van Vuuren, D. P., Eickhout, B., and Lelieveld, J.: Impact of future land use and land cover changes on atmospheric chemistry-climate interactions, *J. Geophys. Res.*, 115, D23301, doi:10.1029/2010jd014041, 2010.
- Gasser, T. and Ciais, P.: A theoretical framework for the net land-to-atmosphere CO₂ flux and its implications in the definition of “emissions from land-use change”, *Earth Syst. Dynam.*, 4, 171–186, doi:10.5194/esd-4-171-2013, 2013.
- Gent, P. R., Danabasoglu, G., Donner, L. J., Holland, M. M., Hunke, E. C., Jayne, S. R., Lawrence, D. M., Neale, R. B., Rasch, P. J., Vertenstein, M., Worley, P. H., Yang, Z.-L., and Zhang, M.: The Community Climate System Model Version 4, *J. Climate*, 24, 4973–4991, doi:10.1175/2011JCLI4083.1, 2011.
- Ginoux, P., Prospero, J. M., Gill, T. E., Hsu, N. C., and Zhao, M.: Global-scale attribution of anthropogenic and natural dust sources and their emission rates based on MODIS Deep Blue aerosol products, *Rev. Geophys.*, 50, RG3005, doi:10.1029/2012RG000388, 2012.
- Guenther, A., Karl, T., Harley, P., Wiedinmyer, C., Palmer, P. I., and Geron, C.: Estimates of global terrestrial isoprene emissions using MEGAN (Model of Emissions of Gases and Aerosols from Nature), *Atmos. Chem. Phys.*, 6, 3181–3210, doi:10.5194/acp-6-3181-2006, 2006.
- Guo, L. B. and Gifford, R.: Soil carbon stocks and land use change: a meta analysis, *Glob. Change Biol.*, 8, 345–360, 2002.
- Hansen, J., Sato, M., Ruedy, R., Nazarenko, L., Lacis, A., Schmidt, G. A., Russell, G., Aleinov, I., Bauer, M., Bauer, S., Bell, N., Cairns, B., Canuto, V., Chandler, M., Cheng, Y., Del Genio, A.,

Potential climate forcing of land use and land cover change

D. S. Ward et al.

Title Page

Abstract

Introduction

Conclusions

References

Tables

Figures

⏪

⏩

◀

▶

Back

Close

Full Screen / Esc

Printer-friendly Version

Interactive Discussion

Faluvegi, G., Fleming, E., Friend, A., Hall, T., Jackman, C., Kelley, M., Kiang, N., Koch, D., Lean, J., Lerner, J., Lo, K., Menon, S., Miller, R., Minnis, P., Novakov, T., Oinas, V., Perlwitz, J., Perlwitz, J., Rind, D., Romanou, A., Shindell, D., Stone, P., Sun, S., Tausnev, N., Thresher, D., Wielicki, B., Wong, T., Yao, M., and Zhang, S.: Efficacy of climate forcings, *J. Geophys. Res.-Atmos.*, 110, D18104, doi:10.1029/2005JD005776, 2005.

Hansen, M. C., Potapov, P. V., Moore, R., Hancher, M., Turubanova, S. A., Tyukavina, A., Thau, D., Stehman, S. V., Goetz, S. J., Loveland, T. R., Kommareddy, A., Egorov, A., Chini, L., Justice, C. O., and Townshend, J. R.: High-resolution global maps of 21st-century forest cover change, *Science*, 342, 850–853, doi:10.1126/science.1244693, 2013.

Harris, I., Jones, P. D., Osborn, T. J., and Lister, D. H.: Updated high-resolution grids of monthly climatic observations – the CRU TS3.10 Dataset, *Int. J. Climatol.*, 34, 623–642, doi:10.1002/joc.3711, 2014.

Heald, C. L., Henze, D. K., Horowitz, L. W., Feddema, J., Lamarque, J. F., Guenther, A., Hess, P. G., Vitt, F., Seinfeld, J. H., Goldstein, A. H., and Fung, I.: Predicted change in global secondary organic aerosol concentrations in response to future climate, emissions, and land use change, *J. Geophys. Res.*, 113, D05211, doi:10.1029/2007jd009092, 2008.

Hergoualc’h, K. and Verchot, L. V.: Stocks and fluxes of carbon associated with land use change in Southeast Asian tropical peatlands: a review, *Global Biogeochem. Cy.*, 25, GB2001, doi:10.1029/2009gb003718, 2011.

Houghton, R. A.: The US carbon budget: contributions from land-use change, *Science*, 285, 574–578, doi:10.1126/science.285.5427.574, 1999.

Houghton, R. A.: How well do we know the flux of CO₂ from land-use change?, *Tellus B*, 62, 337–351, doi:10.1111/j.1600-0889.2010.00473.x, 2010.

Houghton, R. A.: Carbon emissions and the drivers of deforestation and forest degradation in the tropics, *Current Opinion in Environmental Sustainability*, 4, 597–603, doi:10.1016/j.cosust.2012.06.006, 2012.

Houghton, R. A., Hobbie, J. E., Melillo, J. M., Moore, B., Peterson, B. J., Shaver, G. R., and Woodwell, G. M.: Changes in the carbon content of the terrestrial biota and soils between 1860 and 1980: a net release of CO₂ to the atmosphere, *Ecol. Monogr.*, 53, 235–262, 1983.

House, J. I., Prentice, I. C., and Le Quéré, C.: Maximum impacts of future reforestation or deforestation on atmospheric CO₂, *Glob. Change Biol.*, 8, 1047–1052, 2002.

Hurrell, J. W., Holland, M. M., Gent, P. R., Ghan, S., Kay, J. E., Kushner, P. J., Lamarque, J. F., Large, W. G., Lawrence, D., Lindsay, K., Lipscomb, W. H., Long, M. C., Mahowald, N.,

Potential climate forcing of land use and land cover change

D. S. Ward et al.

Title Page

Abstract

Introduction

Conclusions

References

Tables

Figures

⏪

⏩

◀

▶

Back

Close

Full Screen / Esc

Printer-friendly Version

Interactive Discussion

Marsh, D. R., Neale, R. B., Rasch, P., Vavrus, S., Vertenstein, M., Bader, D., Collins, W. D., Hack, J. J., Kiehl, J., and Marshall, S.: The Community Earth System Model: a framework for collaborative research, *B. Am. Meteorol. Soc.*, 94, 1339–1360, doi:10.1175/BAMS-D-12-00121.1, 2013.

5 Hurtt, G. C., Chini, L. P., Frohking, S., Betts, R. A., Feddema, J., Fischer, G., Fisk, J. P., Hibbard, K., Houghton, R. A., Janetos, A., Jones, C. D., Kindermann, G., Kinoshita, T., Klein Goldewijk, K., Riahi, K., Shevliakova, E., Smith, S., Stehfest, E., Thomson, A., Thornton, P., Vuuren, D. P., and Wang, Y. P.: Harmonization of land-use scenarios for the period 1500–2100: 600 years of global gridded annual land-use transitions, wood harvest, and resulting secondary lands, *Climatic Change*, 109, 117–161, doi:10.1007/s10584-011-0153-2, 2011.

10 Jones, A. D., Collins, W. D., and Torn, M. S.: On the additivity of radiative forcing between land use change and greenhouse gases, *Geophys. Res. Lett.*, 40, 4036–4041, doi:10.1002/grl.50754, 2013.

15 Jones, C., Robertson, E., Arora, V., Friedlingstein, P., Shevliakova, E., Bopp, L., Brovkin, V., Hajima, T., Kato, E., Kawamiya, M., Liddicoat, S., Lindsay, K., Reick, C. H., Roelandt, C., Segschneider, J., and Tjiputra, J.: Twenty-first-century compatible CO₂ emissions and airborne fraction simulated by CMIP5 Earth System Models under four representative concentration pathways, *J. Climate*, 26, 4398–4413, doi:10.1175/jcli-d-12-00554.1, 2013.

20 Kloster, S., Mahowald, N. M., Randerson, J. T., Thornton, P. E., Hoffman, F. M., Levis, S., Lawrence, P. J., Feddema, J. J., Oleson, K. W., and Lawrence, D. M.: Fire dynamics during the 20th century simulated by the Community Land Model, *Biogeosciences*, 7, 1877–1902, doi:10.5194/bg-7-1877-2010, 2010.

Kloster, S., Mahowald, N. M., Randerson, J. T., and Lawrence, P. J.: The impacts of climate, land use, and demography on fires during the 21st century simulated by CLM-CN, *Biogeosciences*, 9, 509–525, doi:10.5194/bg-9-509-2012, 2012.

25 Kroeze, C., Mosier, A., and Bouwman, L.: Closing the global N₂O budget: a retrospective analysis 1500–1994, *Global Biogeochem. Cy.*, 13, 1–8, 1999.

Lal, R.: Soil carbon sequestration impacts on global climate change and food security, *Science*, 304, 1623–1627, doi:10.1126/science.1097396, 2004.

30 Lamarque, J.-F., Kiehl, J. T., Brasseur, G. P., Butler, T., Cameron-Smith, P., Collins, W. D., Collins, W. J., Granier, C., Hauglustaine, D., Hess, P. G., Holland, E. A., Horowitz, L., Lawrence, M. G., McKenna, D., Merilees, P., Prather, M. J., Rasch, P. J., Rotman, D., Shindell, D., and Thornton, P.: Assessing future nitrogen deposition and carbon cycle feedback

Potential climate forcing of land use and land cover change

D. S. Ward et al.

Title Page

Abstract

Introduction

Conclusions

References

Tables

Figures

◀

▶

◀

▶

Back

Close

Full Screen / Esc

Printer-friendly Version

Interactive Discussion

using a multimodel approach: analysis of nitrogen deposition, *J. Geophys. Res.-Atmos.*, 110, D19303, doi:10.1029/2005JD005825, 2005.

Lamarque, J.-F., Bond, T. C., Eyring, V., Granier, C., Heil, A., Klimont, Z., Lee, D., Liousse, C., Mieville, A., Owen, B., Schultz, M. G., Shindell, D., Smith, S. J., Stehfest, E., Van Aardenne, J., Cooper, O. R., Kainuma, M., Mahowald, N., McConnell, J. R., Naik, V., Riahi, K., and van Vuuren, D. P.: Historical (1850–2000) gridded anthropogenic and biomass burning emissions of reactive gases and aerosols: methodology and application, *Atmos. Chem. Phys.*, 10, 7017–7039, doi:10.5194/acp-10-7017-2010, 2010.

Lawrence, P. J. and Chase, T. N.: Investigating the climate impacts of global land cover change in the community climate system model, *Int. J. Climatol.*, 30, 2066–2087, doi:10.1002/joc.2061, 2010.

Lawrence, P. J., Feddema, J. J., Bonan, G. B., Meehl, G. A., O'Neill, B. C., Oleson, K. W., Levis, S., Lawrence, D. M., Kluzek, E., Lindsay, K., and Thornton, P. E.: Simulating the biogeochemical and biogeophysical impacts of transient land cover change and wood harvest in the Community Climate System Model (CCSM4) from 1850 to 2100, *J. Climate*, 25, 3071–3095, doi:10.1175/jcli-d-11-00256.1, 2012.

Liu, X., Xie, S., Boyle, J., Klein, S. A., Shi, X., Wang, Z., Lin, W., Ghan, S. J., Earle, M., Liu, P. S. K., and Zelenyuk, A.: Testing cloud microphysics parameterizations in NCAR CAM5 with ISDAC and M-PACE observations, *J. Geophys. Res.-Atmos.*, 116, D00T11, doi:10.1029/2011JD015889, 2011.

Liu, X., Easter, R. C., Ghan, S. J., Zaveri, R., Rasch, P., Shi, X., Lamarque, J.-F., Gettelman, A., Morrison, H., Vitt, F., Conley, A., Park, S., Neale, R., Hannay, C., Ekman, A. M. L., Hess, P., Mahowald, N., Collins, W., Iacono, M. J., Bretherton, C. S., Flanner, M. G., and Mitchell, D.: Toward a minimal representation of aerosols in climate models: description and evaluation in the Community Atmosphere Model CAM5, *Geosci. Model Dev.*, 5, 709–739, doi:10.5194/gmd-5-709-2012, 2012.

Lohmann, U. and Feichter, J.: Global indirect aerosol effects: a review, *Atmos. Chem. Phys.*, 5, 715–737, doi:10.5194/acp-5-715-2005, 2005.

Mahowald, N. M.: Aerosol indirect effect on biogeochemical cycles and climate, *Science*, 334, 794–796, doi:10.1126/science.1207374, 2011.

Mahowald, N. M., Muhs, D. R., Levis, S., Rasch, P. J., Yoshioka, M., Zender, C. S., and Luo, C.: Change in atmospheric mineral aerosols in response to climate: last glacial period, prein-

Potential climate forcing of land use and land cover change

D. S. Ward et al.

Title Page

Abstract

Introduction

Conclusions

References

Tables

Figures

⏪

⏩

◀

▶

Back

Close

Full Screen / Esc

Printer-friendly Version

Interactive Discussion

dustrial, modern, and doubled carbon dioxide climates, *J. Geophys. Res.*, 111, D10202, doi:10.1029/2005jd006653, 2006.

Mahowald, N. M., Ward, D. S., Kloster, S., Flanner, M. G., Heald, C. L., Heavens, N. G., Hess, P. G., Lamarque, J.-F., and Chuang, P. Y.: Aerosol impacts on climate and biogeochemistry, *Annu. Rev. Env. Resour.*, 36, 45–74, doi:10.1146/annurev-environ-042009-094507, 2011.

Marlon, J. R., Bartlein, P. J., Carcaillet, C., Gavin, D. G., Harrison, S. P., Higuera, P. E., Joos, F., Power, M. J., and Prentice, I. C.: Climate and human influences on global biomass burning over the past two millennia, *Nat. Geosci.*, 1, 697–702, doi:10.1038/ngeo313, 2008.

Matthews, H. D., Weaver, A. J., Meissner, K. J., Gillett, N. P., and Eby, M.: Natural and anthropogenic climate change: incorporating historical land cover change, vegetation dynamics and the global carbon cycle, *Clim. Dynam.*, 22, 461–479 doi:10.1007/s00382-004-0392-2, 2004.

Meinshausen, M., Meinshausen, N., Hare, W., Raper, S. C., Frieler, K., Knutti, R., Frame, D. J., and Allen, M. R.: Greenhouse-gas emission targets for limiting global warming to 2 degrees C, *Nature*, 458, 1158–1162, doi:10.1038/nature08017, 2009.

Meinshausen, M., Raper, S. C. B., and Wigley, T. M. L.: Emulating coupled atmosphere–ocean and carbon cycle models with a simpler model, MAGICC6 – Part 1: Model description and calibration, *Atmos. Chem. Phys.*, 11, 1417–1456, doi:10.5194/acp-11-1417-2011, 2011a.

Meinshausen, M., Smith, S. J., Calvin, K., Daniel, J. S., Kainuma, M. L. T., Lamarque, J. F., Matsumoto, K., Montzka, S. A., Raper, S. C. B., Riahi, K., Thomson, A., Velders, G. J. M., and Vuuren, D. P. P.: The RCP greenhouse gas concentrations and their extensions from 1765 to 2300, *Climatic Change*, 109, 213–241, doi:10.1007/s10584-011-0156-z, 2011b.

Meyfroidt, P. and Lambin, E. F.: Global forest transition: prospects for an end to deforestation, *Annu. Rev. Env. Resour.*, 36, 343–371, doi:10.1146/annurev-environ-090710-143732, 2011.

Morrison, H. and Gettelman, A.: A new two-moment bulk stratiform cloud microphysics scheme in the Community Atmosphere Model, Version 3 (CAM3). Part I: Description and numerical tests, *J. Climate*, 21, 3642–3659, doi:10.1175/2008JCLI2105.1, 2008.

Moss, R. H., Edmonds, J. A., Hibbard, K. A., Manning, M. R., Rose, S. K., van Vuuren, D. P., Carter, T. R., Emori, S., Kainuma, M., Kram, T., Meehl, G. A., Mitchell, J. F., Nakicenovic, N., Riahi, K., Smith, S. J., Stouffer, R. J., Thomson, A. M., Weyant, J. P., and Wilbanks, T. J.: The next generation of scenarios for climate change research and assessment, *Nature*, 463, 747–756, doi:10.1038/nature08823, 2010.

Potential climate forcing of land use and land cover change

D. S. Ward et al.

Title Page

Abstract

Introduction

Conclusions

References

Tables

Figures

◀

▶

◀

▶

Back

Close

Full Screen / Esc

Printer-friendly Version

Interactive Discussion

- Myhre, G., Kvalevåg, M. M., and Schaaf, C. B.: Radiative forcing due to anthropogenic vegetation change based on MODIS surface albedo data, *Geophys. Res. Lett.*, 32, L21410, doi:10.1029/2005gl024004, 2005.
- Myhre, G., Shindell, D., Breon, F.-M., Collins, W., Fuglestedt, J., Huang, J., Koch, D., Lamarque, J. F., Lee, D., Mendoza, B., Nakajima, T., Robock, A., Stephens, G., Takemura, T., and Zhang, H.: Anthropogenic and natural radiative forcing, in: *Climate Change 2013: The Physical Science Basis, Contribution of Working Group I to the Fifth Assessment Report of the Intergovernmental Panel on Climate Change*, edited by: Stocker, T. F., Qin, D., Plattner, G.-K., Tignor, M., Allen, S. K., Boschung, J., Nauels, A., Xia, Y., Bex, V., and Midgley, P. M., Cambridge University Press, New York, NY, USA, 659–740, 2013.
- Naik, V., Mauzerall, D., Horowitz, L., Schwarzkopf, M. D., Ramaswamy, V., and Oppenheimer, M.: Net radiative forcing due to changes in regional emissions of tropospheric ozone precursors, *J. Geophys. Res.*, 110, D24306, doi:10.1029/2005jd005908, 2005.
- O'Halloran, T. L., Law, B. E., Goulden, M. L., Wang, Z., Barr, J. G., Schaaf, C., Brown, M., Fuentes, J. D., Göckede, M., Black, A., and Engel, V.: Radiative forcing of natural forest disturbances, *Glob. Change Biol.*, 18, 555–565, doi:10.1111/j.1365-2486.2011.02577.x, 2012.
- Oleson, K. W., Niu, G. Y., Yang, Z. L., Lawrence, D. M., Thornton, P. E., Lawrence, P. J., Stöckli, R., Dickinson, R. E., Bonan, G. B., Levis, S., Dai, A., and Qian, T.: Improvements to the Community Land Model and their impact on the hydrological cycle, *J. Geophys. Res.*, 113, G01021, doi:10.1029/2007jg000563, 2008.
- Pielke, R. A., Marland, G., Betts, R. A., Chase, T. N., Eastman, J. L., Niles, J. O., Niyogi, D. S., and Running, S. W.: The influence of land-use change and landscape dynamics on the climate system: relevance to climate-change policy beyond the radiative effect of greenhouse gases, *Philos. T. R. Soc. A*, 360, 1705–1719, 2002.
- Pitman, A. J., de Noblet-Ducoudré, N., Cruz, F. T., Davin, E. L., Bonan, G. B., Brovkin, V., Claussen, M., Delire, C., Ganzeveld, L., Gayler, V., van den Hurk, B. J. J. M., Lawrence, P. J., van der Molen, M. K., Müller, C., Reick, C. H., Seneviratne, S. I., Strengers, B. J., and Voldoire, A.: Uncertainties in climate responses to past land cover change: first results from the LUCID intercomparison study, *Geophys. Res. Lett.*, 36, L14814, doi:10.1029/2009gl039076, 2009.
- Pongratz, J., Reick, C., Raddatz, T., and Claussen, M.: A reconstruction of global agricultural areas and land cover for the last millennium, *Global Biogeochem. Cy.*, 22, GB3018, doi:10.1029/2007gb003153, 2008.

Potential climate forcing of land use and land cover change

D. S. Ward et al.

Title Page

Abstract

Introduction

Conclusions

References

Tables

Figures

◀

▶

◀

▶

Back

Close

Full Screen / Esc

Printer-friendly Version

Interactive Discussion

Pongratz, J., Raddatz, T., Reick, C. H., Esch, M., and Claussen, M.: Radiative forcing from anthropogenic land cover change since A. D. 800, *Geophys. Res. Lett.*, 36, L02709, doi:10.1029/2008gl036394, 2009.

Prather, M., Ehhalt, D., Dentener, F., Derwent, R., Dlugokencky, E. J., Holland, E., Isaksen, I., Katima, J., Kirchhoff, V., Matson, P., Midgley, P., and Wang, M.: Atmospheric chemistry and greenhouse gases, in: *Climate Change 2001: The Scientific Basis*, edited by: Houghton, J. T., Ding, Y., Griggs, D. J., Noguer, M., Van der Linden, P. J., Dai, X., Maskell, K., and Johnson, C. A., Intergovernmental Panel on Climate Change, Cambridge University Press, Cambridge, 239–287, 2001.

Ramankutty, N., Foley, J. A., Norman, J., and McSweeney, K.: The global distribution of cultivable lands: current patterns and sensitivity to possible climate change, *Global. Ecol. Biogeogr.*, 11, 377–392, doi:10.1046/j.1466-822x.2002.00294.x, 2002.

Ramankutty, N., Evan, A. T., Monfreda, C., and Foley, J. A.: Farming the planet: 1. Geographic distribution of global agricultural lands in the year 2000, *Global Biogeochem. Cy.*, 22, GB1003, doi:10.1029/2007GB002952, 2008.

Ramaswamy, V., Boucher, O., Haigh, J., Hauglustine, D., Haywood, J., Myhre, G., Nakajima, T., Shi, G., and Solomon, S.: Radiative forcing of climate, in: *Climate Change 2001: The Scientific Basis*, edited by: Houghton, J. T., Ding, Y., Griggs, D. J., Noguer, M., Van der Linden, P. J., Dai, X., Maskell, K., and Johnson, C. A., Intergovernmental Panel on Climate Change, Cambridge University Press, Cambridge, UK, 349–416, 2001.

Randerson, J. T., Liu, H., Flanner, M. G., Chambers, S. D., Jin, Y., Hess, P. G., Pfister, G., Mack, M. C., Treseder, K. K., Welp, L. R., Chapin, F. S., Harden, J. W., Goulden, M. L., Lyons, E., Neff, J. C., Schuur, E. A., and Zender, C. S.: The impact of boreal forest fire on climate warming, *Science*, 314, 1130–1132, doi:10.1126/science.1132075, 2006.

Reay, D. S., Davidson, E. A., Smith, K. A., Smith, P., Melillo, J. M., Dentener, F., and Crutzen, P. J.: Global agriculture and nitrous oxide emissions, *Nature Climate Change*, 2, 410–416, 2012.

Riahi, K., Grübler, A., and Nakicenovic, N.: Scenarios of long-term socio-economic and environmental development under climate stabilization, *Technol. Forecast. Soc.*, 74, 887–935, doi:10.1016/j.techfore.2006.05.026, 2007.

Rulli, M. C., Savioli, A., and D'Odorico, P.: Global land and water grabbing, *P. Natl. Acad. Sci. USA*, 110, 892–897, doi:10.1073/pnas.1213163110, 2013.

Potential climate forcing of land use and land cover change

D. S. Ward et al.

Title Page

Abstract

Introduction

Conclusions

References

Tables

Figures

◀

▶

◀

▶

Back

Close

Full Screen / Esc

Printer-friendly Version

Interactive Discussion

- Runyan, C. W., D'Odorico, P., and Lawrence, D.: Physical and biological feedbacks of deforestation, *Rev. Geophys.*, 50, RG4006, doi:10.1029/2012rg000394, 2012.
- Shevliakova, E., Pacala, S. W., Malyshev, S., Hurtt, G. C., Milly, P. C. D., Caspersen, J. P., Sentman, L. T., Fisk, J. P., Wirth, C., and Crevoisier, C.: Carbon cycling under 300 years of land use change: importance of the secondary vegetation sink, *Global Biogeochem. Cy.*, 23, GB2022, doi:10.1029/2007gb003176, 2009.
- Shindell, D. T., Faluvegi, G., Koch, D. M., Schmidt, G. A., Unger, N., and Bauer, S. E.: Improved attribution of climate forcing to emissions, *Science*, 326, 716–718, doi:10.1126/science.1174760, 2009.
- Shine, K. P., Berntsen, T. K., Fuglestvedt, J. S., Skeie, R. B., and Stuber, N.: Comparing the climate effect of emissions of short- and long-lived climate agents, *Philos. T. R. Soc. A*, 365, 1903–1914, doi:10.1098/rsta.2007.2050, 2007.
- Sitch, S., Brovkin, V., von Bloh, W., van Vuuren, D., Eickhout, B., and Ganopolski, A.: Impacts of future land cover changes on atmospheric CO₂ and climate, *Global Biogeochem. Cy.*, 19, GB2013, doi:10.1029/2004gb002311, 2005.
- Skeie, R. B., Berntsen, T. K., Myhre, G., Tanaka, K., Kvalevåg, M. M., and Hoyle, C. R.: Anthropogenic radiative forcing time series from pre-industrial times until 2010, *Atmos. Chem. Phys.*, 11, 11827–11857, doi:10.5194/acp-11-11827-2011, 2011.
- Stöckli, R., Lawrence, D. M., Niu, G. Y., Oleson, K. W., Thornton, P. E., Yang, Z. L., Bonan, G. B., Denning, A. S., and Running, S. W.: Use of FLUXNET in the Community Land Model development, *J. Geophys. Res.-Biogeo.*, 113, G01025, doi:10.1029/2007JG000562, 2008.
- Strassmann, K. M., Joos, F., and Fischer, G.: Simulating effects of land use changes on carbon fluxes: past contributions to atmospheric CO₂ increases and future commitments due to losses of terrestrial sink capacity, *Tellus B*, 60, 583–603, doi:10.1111/j.1600-0889.2008.00340.x, 2008.
- Strengers, B. J., Müller, C., Schaeffer, M., Haarsma, R. J., Severijns, C., Gerten, D., Schaphoff, S., van den Houdt, R., and Oostenrijk, R.: Assessing 20th century climate-vegetation feedbacks of land-use change and natural vegetation dynamics in a fully coupled vegetation-climate model, *Int. J. Climatol.*, 30, 2055–2065, doi:10.1002/joc.2132, 2010.
- Syakila, A. and Kroeze, C.: The global nitrous oxide budget revisited, *Greenhouse Gas Measurement and Management*, 1, 17–26, doi:10.3763/ghgmm.2010.0007, 2011.
- Taylor, K. E., Stouffer, R. J., and Meehl, G. A.: An overview of CMIP5 and the experiment design, *B. Am. Meteorol. Soc.*, 93, 485–498, doi:10.1175/bams-d-11-00094.1, 2012.

Potential climate forcing of land use and land cover change

D. S. Ward et al.

Title Page

Abstract

Introduction

Conclusions

References

Tables

Figures

◀

▶

◀

▶

Back

Close

Full Screen / Esc

Printer-friendly Version

Interactive Discussion



- Thornton, P. E., Doney, S. C., Lindsay, K., Moore, J. K., Mahowald, N., Randerson, J. T., Fung, I., Lamarque, J.-F., Feddema, J. J., and Lee, Y.-H.: Carbon-nitrogen interactions regulate climate-carbon cycle feedbacks: results from an atmosphere–ocean general circulation model, *Biogeosciences*, 6, 2099–2120, doi:10.5194/bg-6-2099-2009, 2009.
- 5 Tubiello, F. N., Salvatore, M., Rossi, S., Ferrara, A., Fitton, N., and Smith, P.: The FAOSTAT database of greenhouse gas emissions from agriculture, *Environ. Res. Lett.*, 8, 015009, doi:10.1088/1748-9326/8/1/015009, 2013.
- Unger, N., Bond, T. C., Wang, J. S., Koch, D. M., Menon, S., Shindell, D. T., and Bauer, S.: Attribution of climate forcing to economic sectors, *P. Natl. Acad. Sci. USA*, 107, 3382–3387, doi:10.1073/pnas.0906548107, 2010.
- 10 van Vuuren, D. P., Elzen, M. G. J., Lucas, P. L., Eickhout, B., Strengers, B. J., Ruijven, B., Wonink, S., and Houdt, R.: Stabilizing greenhouse gas concentrations at low levels: an assessment of reduction strategies and costs, *Climatic Change*, 81, 119–159, doi:10.1007/s10584-006-9172-9, 2007.
- 15 van Vuuren, D. P., Edmonds, J., Kainuma, M., Riahi, K., Thomson, A., Hibbard, K., Hurtt, G. C., Kram, T., Krey, V., Lamarque, J.-F., Masui, T., Meinshausen, M., Nakicenovic, N., Smith, S. J., and Rose, S. K.: The representative concentration pathways: an overview, *Climatic Change*, 109, 5–31, doi:10.1007/s10584-011-0148-z, 2011.
- Wang, M., Ghan, S., Ovchinnikov, M., Liu, X., Easter, R., Kassianov, E., Qian, Y., and Morrison, H.: Aerosol indirect effects in a multi-scale aerosol-climate model PNNL-MMF, *Atmos. Chem. Phys.*, 11, 5431–5455, doi:10.5194/acp-11-5431-2011, 2011.
- 20 Ward, D. S., Kloster, S., Mahowald, N. M., Rogers, B. M., Randerson, J. T., and Hess, P. G.: The changing radiative forcing of fires: global model estimates for past, present and future, *Atmos. Chem. Phys.*, 12, 10857–10886, doi:10.5194/acp-12-10857-2012, 2012.
- 25 Willmott, C. J. and Feddema, J. J.: A more rational climatic moisture index*, *Prof. Geogr.*, 44, 84–88, 1992.
- Wise, M., Calvin, K., Thomson, A., Clarke, L., Bond-Lamberty, B., Sands, R., Smith, S. J., Janetos, A., and Edmonds, J.: Implications of limiting CO₂ concentrations for land use and energy, *Science*, 324, 1183–1186, doi:10.1126/science.1168475, 2009.
- 30 Wu, S., Mickley, L. J., Kaplan, J. O., and Jacob, D. J.: Impacts of changes in land use and land cover on atmospheric chemistry and air quality over the 21st century, *Atmos. Chem. Phys.*, 12, 1597–1609, doi:10.5194/acp-12-1597-2012, 2012.

Zaehle, S., Ciais, P., Friend, A. D., and Prieur, V.: Carbon benefits of anthropogenic reactive nitrogen offset by nitrous oxide emissions, *Nat. Geosci.*, 4, 601–605, 2011.

ACPD

14, 12167–12234, 2014

Potential climate forcing of land use and land cover change

D. S. Ward et al.

Title Page

Abstract

Introduction

Conclusions

References

Tables

Figures



Back

Close

Full Screen / Esc

Printer-friendly Version

Interactive Discussion



Potential climate forcing of land use and land cover change

D. S. Ward et al.

Title Page

Abstract

Introduction

Conclusions

References

Tables

Figures

◀

▶

◀

▶

Back

Close

Full Screen / Esc

Printer-friendly Version

Interactive Discussion

Table 1. Summary outline of Sect. 3.

Section	Topic	Summary
3.1	LULCC Activities	–
3.1.1	LCC and wood harvesting	These processes simulated in CLM3 (LCC: land cover change)
3.1.2	Fires	Changes in global fires from LULCC simulated by CLM3
3.1.3	Agricultural activities	Fertilizer, soil modification, livestock, rice cultivation and waste burning
3.2	Emissions	Non-LULCC emissions from ACCMIP and van Vuuren et al. (2011)
3.2.1	Agricultural emissions	Historical emissions from ACCMIP, RCPs from van Vuuren et al. (2011)
3.2.2	Fire emissions	Emissions factors applied to changes in fire activity from CLM3
3.2.3	Dust emissions	Cultivated area used to modify soil erodibility and resulting dust emissions
3.2.4	SOA emissions	Computed offline with MEGAN using LULCC leaf area changes from CLM3
3.2.5	CO ₂ emissions	Difference in terrestrial C storage in CLM3 with and without LULCC
3.2.6	N ₂ O emissions	Emissions scaled by changes in crop and pasture area
3.3	Concentration changes	–
3.3.1	Tropospheric O ₃ conc.	Concentration changes simulated by CAM4 with year 2000 climate
3.3.2	CH ₄ concentration	Direct and indirect changes computed using methods of Ward et al. (2012)
3.3.3	CO ₂ concentration	Pulse response function with approximated fertilization feedback included
3.3.4	N ₂ O concentration	Box model approach from Kroeze et al. (1999)
3.3.5	Aerosols concentrations	Simulated by CAM5 with MAM3, four year simulations (post-spinup)
3.4	RF calculations	Future LULCC RFs are computed against a RCP4.5 background atmosphere
3.4.1	Tropospheric O ₃ RF	Computed offline with the Parallel Offline Radiative Transfer (PORT) tool
3.4.2	CO ₂ , CH ₄ , N ₂ O RFs	Computed with simple expressions from Ramaswamy et al. (2001)
3.4.3	Aerosol effects	Simulated by CAM5 and scaled to the estimates of Forster et al. (2007)
3.4.4	Land surface albedo	Computed from albedo change simulated by CLM3 for LULCC
3.4.5	Aerosol bgc feedbacks	Changes to CO ₂ conc. from biogeochemical feedbacks (Mahowald, 2011)
3.5	Uncertainty	See Appendix A for details of uncertainty calculations

Potential climate forcing of land use and land cover change

D. S. Ward et al.

Title Page

Abstract

Introduction

Conclusions

References

Tables

Figures

⏪

⏩

◀

▶

Back

Close

Full Screen / Esc

Printer-friendly Version

Interactive Discussion



Table 4. RFs for the year 2010 and the year 2100 compared to van Vuuren et al. (2011). For year 2100 we show the RF from RCP4.5 scenario emissions (referenced to year 1850) estimated from the modeling results in this study and from van Vuuren et al. (2011) given in Wm^{-2} . Note, as stated in the main text, the total aerosol direct and indirect RFs for the year 2010 are from the IPCC model consensus with only the partitioning between LULCC and other anthropogenic activities (FF+) determined by the modeling results of this study and the same scaling is applied to the year 2100 aerosol RFs.

	LULCC	FF+	Total	Van Vuuren et al. (2011)
2010				
Total RF	0.88	1.05	1.93	1.95
CO ₂ RF	0.43	1.35	1.78	1.69
CH ₄ RF	0.3	0.14	0.44	0.44
N ₂ O RF	0.14	0.03	0.17	0.16
Halocarbons	0	0.34	0.34	0.34
Aerosols/O ₃ /alb*	0.01	-0.81	-0.8	-0.68
2100-RCP4.5				
Total RF	0.95	3.34	4.29	4.14
CO ₂ RF	0.31	3.16	3.47	3.47
CH ₄ RF	0.31	0.12	0.43	0.37
N ₂ O RF	0.18	0.12	0.3	0.31
Halocarbons	0	0.18	0.18	0.18
Aerosols/O ₃ /alb*	0.15	-0.24	-0.09	-0.19

* This sum RF includes aerosols (direct effects, indirect effects on clouds, and deposition onto snow/ice surfaces), tropospheric O₃ and forcing from surface albedo changes.

Potential climate forcing of land use and land cover change

D. S. Ward et al.

Title Page

Abstract

Introduction

Conclusions

References

Tables

Figures

⏪

⏩

◀

▶

Back

Close

Full Screen / Esc

Printer-friendly Version

Interactive Discussion

Table 5. Quantiles of the spatial distribution of the different forcings from historical LULCC (assessed in 2010) when represented as a probability density function. The grid spacing is 1.9° latitude by 2.5° longitude. Note that we show AOD in place of the aerosol forcings since the distribution of these forcings includes variability in cloud properties that are not directly attributable to changes in aerosols at this grid spacing.

Forcing	Mean	Quantiles						
		Min.	$q_{0.1}$	$q_{0.25}$	Median	$q_{0.75}$	$q_{0.9}$	Max.
CO ₂	0.43 [±0.27]	0.43	0.43	0.43	0.43	0.43	0.43	0.43
N ₂ O	0.14 [±0.04]	0.14	0.14	0.14	0.14	0.14	0.14	0.14
CH ₄	0.30 [±0.07]	0.3	0.3	0.3	0.3	0.3	0.3	0.3
Ozone	0.12 [±0.18]	−0.10	0.06	0.08	0.11	0.15	0.19	0.37
Albedo*	−0.05 [±0.12]	−5.6	−0.45	−0.09	0	0	0.08	2.5
Ice alb.*	0.01 [±0.02]	−1.52	−0.01	0	0	0.01	0.06	2.6
AOD	0.005	−0.18	−0.02	0	0.03	0.07	0.11	0.29

* The spatial distribution of the RF from albedo changes is computed only for land points.

Potential climate forcing of land use and land cover change

D. S. Ward et al.

Title Page

Abstract

Introduction

Conclusions

References

Tables

Figures

⏪

⏩

◀

▶

Back

Close

Full Screen / Esc

Printer-friendly Version

Interactive Discussion



Table 6. Enhancement of CO₂ RF by other forcing agents for LULCC and other anthropogenic activities (FF+). RFs are given in units of W m⁻².

Scenario	LULCC		FF+ ^a		Enhancement ^b
	CO ₂ RF	TOTAL RF	CO ₂ RF	TOTAL RF	
2010	0.43	0.88	1.35	1.05	2.6
RCP2.6	0.51	1.08	3.14	3.14	2.1
RCP4.5	0.31	0.96	3.14	3.14	3.1
RCP6.0	0.54	1.21	3.14	3.14	2.2
RCP8.5	0.81	2.25	3.14	3.14	2.8
WCS ^c	1.58	4.58	3.14	3.14	2.9

^a Other anthropogenic activities, dominated by fossil fuel burning, and including the aerosol effects RFs from the IPCC AR4 (Forster et al., 2007).

^b Enhancement is defined as the ratio of total RF to CO₂ RF for LULCC divided by the ratio of total RF to CO₂ RF for FF+.

^c Worst case scenario.

Potential climate forcing of land use and land cover change

D. S. Ward et al.

Table A1. Values for the three types of uncertainty calculated in this study. Uncertainty due to fires is specific to each future LULCC scenario and for other future anthropogenic activities (FF+).

Forcing	Model [Wm ⁻²]	Partitioning [%]	Fire [Wm ⁻²]					
			RCP2.6	RCP4.5	RCP6.0	RCP8.5	WCS*	FF+
CO ₂	±0.10	±15	±0.04	±0.02	±0.04	±0.05	±0.15	0
N ₂ O	±0.01	±25	0	0	0	0	0	0
CH ₄	±0.03	±15	±0.01	±0.01	±0.01	±0.01	±0.02	±0.02
Ozone	+0.18, -0.06	±40	0	0	0	0	±0.01	±0.01
Aero DE	±0.24	±40	0	±0.02	±0.02	±0.02	±0.1	±0.1
Aero IE	+0.24, -0.67	±40	±0.05	±0.02	0	±0.14	±0.23	±0.28
Albedo	±0.12	0	±0.01	±0.01	0	0	±0.01	0
Ice alb.	±0.06	±40	0	±0.01	0	0	0	0
HaloCs	±0.02	0	0	0	0	0	0	0

* Worst case scenario.

[Title Page](#)
[Abstract](#)
[Introduction](#)
[Conclusions](#)
[References](#)
[Tables](#)
[Figures](#)
[⏪](#)
[⏩](#)
[◀](#)
[▶](#)
[Back](#)
[Close](#)
[Full Screen / Esc](#)
[Printer-friendly Version](#)
[Interactive Discussion](#)


Potential climate forcing of land use and land cover change

D. S. Ward et al.

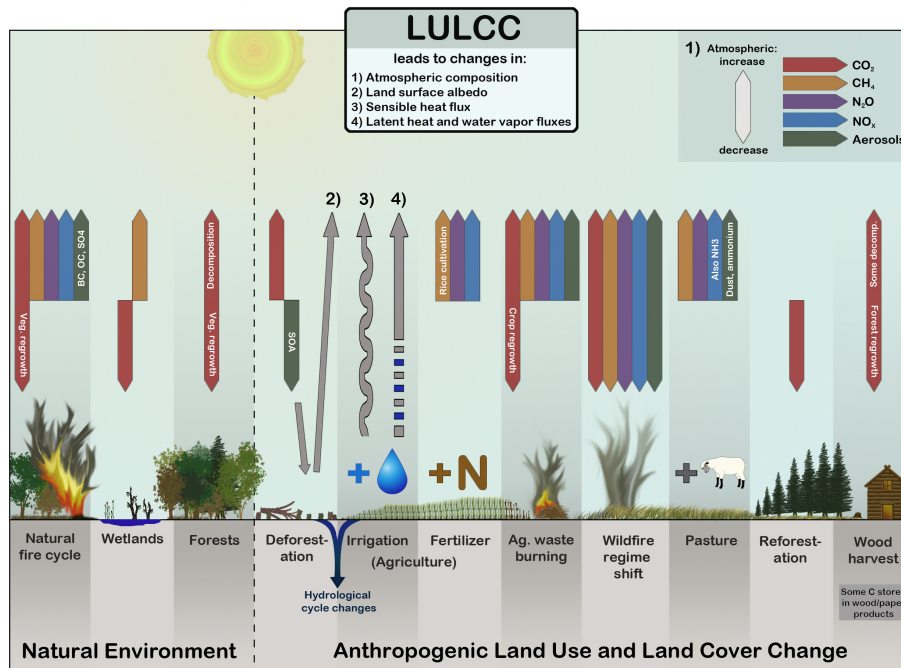


Fig. 1. A schematic illustration of the climate impacts of land use and land cover change. See Fig. 2 for a representation of the processes and emissions included in this study.

Title Page

Abstract Introduction

Conclusions References

Tables Figures

◀ ▶

◀ ▶

Back Close

Full Screen / Esc

Printer-friendly Version

Interactive Discussion

Potential climate forcing of land use and land cover change

D. S. Ward et al.

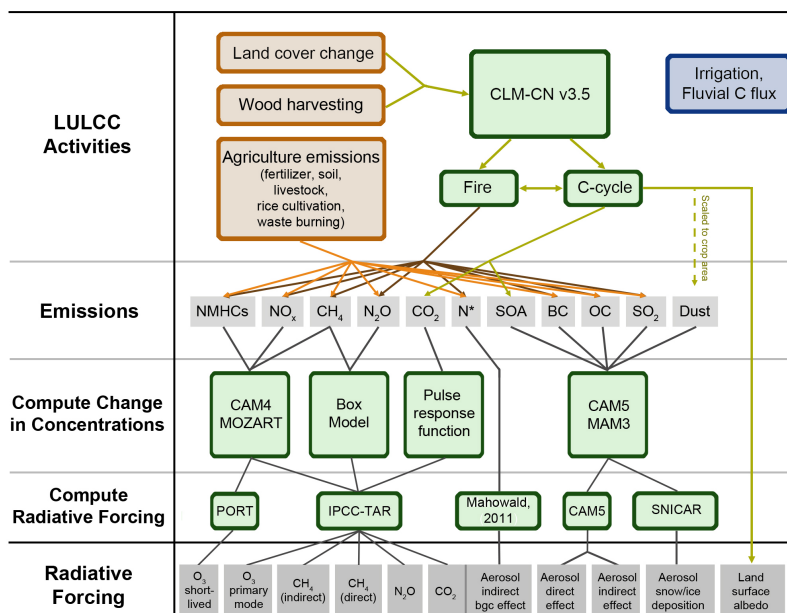


Fig. 2. A flow chart summarizing the methodology used in this study to compute the RF of the various forcing agents of LULCC. The colors of the boxes indicate processes that are independent of this study (orange), processes and computational steps that were completed as part of this study (green), and processes that were not included in this study, but are likely important for climate (blue). Acronyms are defined as follows: CLM-CN (Community Land Model with Carbon/Nitrogen cycles) (Oleson et al., 2008; Stockli et al., 2008), CAM (Community Atmosphere Model) (Gent et al., 2011), MOZART (Model for Ozone and Related Chemical Tracers) (Emmons et al., 2010), PORT (Parallel Offline Radiative Transfer) (Conley et al., 2013), TAR (Third Assessment Report) (Ramaswamy et al., 2001), and SNICAR (Snow Ice and Radiative Aerosol Model) (Flanner and Zender, 2006). * Total nitrogen (N) includes contributions from NH₃, N₂O and NO_x emissions.

Title Page

Abstract Introduction

Conclusions References

Tables Figures

◀ ▶

◀ ▶

Back Close

Full Screen / Esc

Printer-friendly Version

Interactive Discussion

Potential climate forcing of land use and land cover change

D. S. Ward et al.

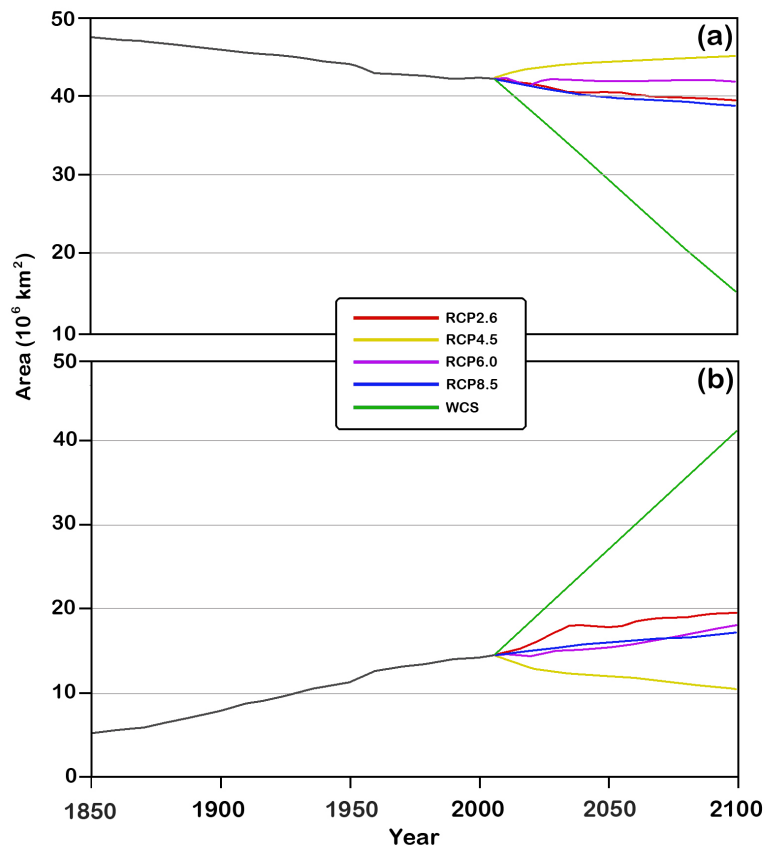


Fig. 3. Change in global total (a) forest and (b) crop areal coverage with time for historical and Representative Concentration Pathway scenarios (Lawrence et al., 2012), and the worst case scenario (WCS; green).

Potential climate forcing of land use and land cover change

D. S. Ward et al.

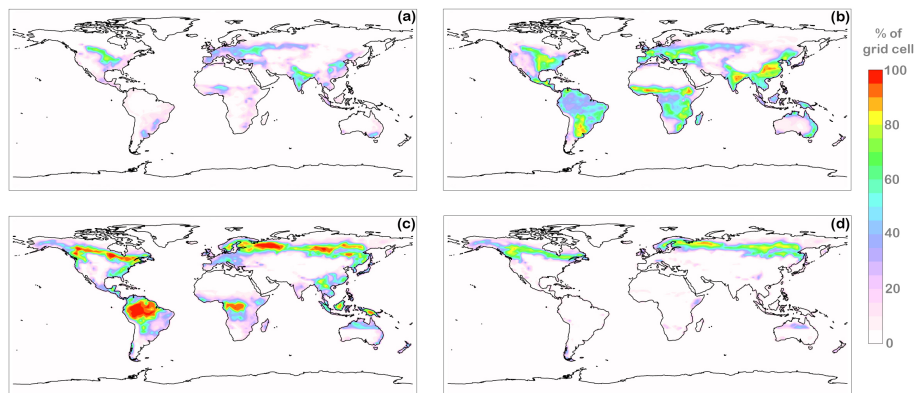


Fig. 4. Percent of gridbox area consisting of **(a)** year 2010 crops, **(b)** potential crops based on climate and soil suitability, **(c)** year 2010 forests, and **(d)** year 2100 forests in the worst case scenario.

[Title Page](#)[Abstract](#)[Introduction](#)[Conclusions](#)[References](#)[Tables](#)[Figures](#)[◀](#)[▶](#)[◀](#)[▶](#)[Back](#)[Close](#)[Full Screen / Esc](#)[Printer-friendly Version](#)[Interactive Discussion](#)

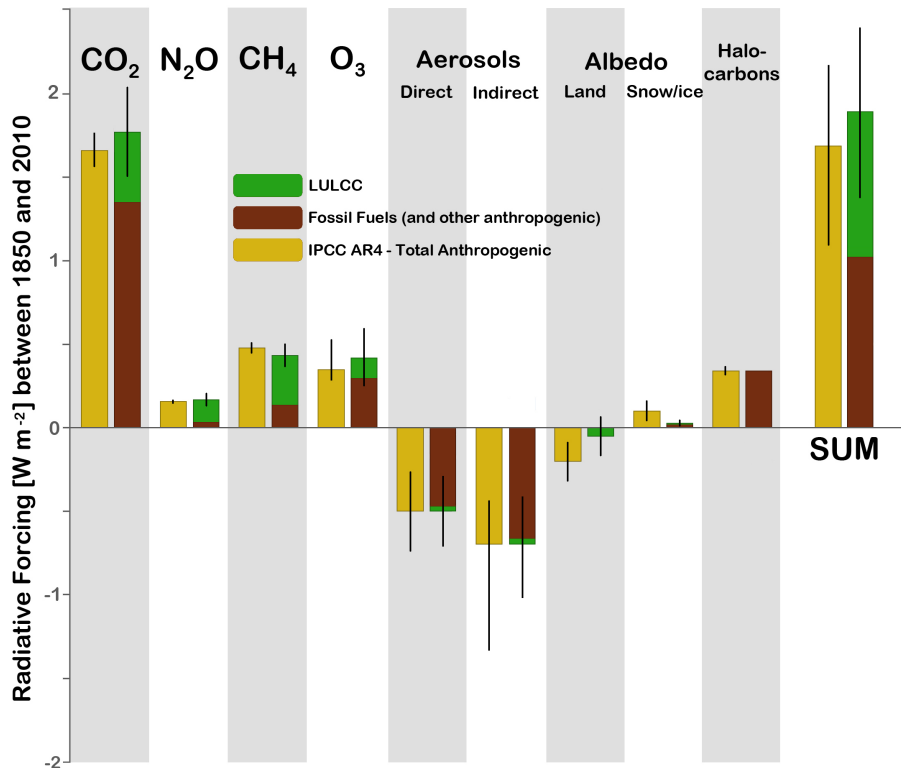


Fig. 5. RFs for LULCC and other anthropogenic impacts estimated by this study for the year 2010 referenced to the year 1850. Total anthropogenic RF from the IPCC AR4 (Forster et al., 2007) are shown for comparison (yellow). Error lines represent one sigma uncertainties in total anthropogenic RF for the IPCC bars and one sigma uncertainties in LULCC RFs as computed in this study (green bars, data given in Table 3). The “SUM” bars show the total RF when all forcing agents are combined. Note that aerosol RFs are scaled to IPCC AR4 values, as explained in the main text.

Potential climate forcing of land use and land cover change

D. S. Ward et al.

Title Page

Abstract Introduction

Conclusions References

Tables Figures

⏪ ⏩

⏴ ⏵

Back Close

Full Screen / Esc

Printer-friendly Version

Interactive Discussion



Potential climate forcing of land use and land cover change

D. S. Ward et al.

Title Page

Abstract

Introduction

Conclusions

References

Tables

Figures

⏪

⏩

◀

▶

Back

Close

Full Screen / Esc

Printer-friendly Version

Interactive Discussion

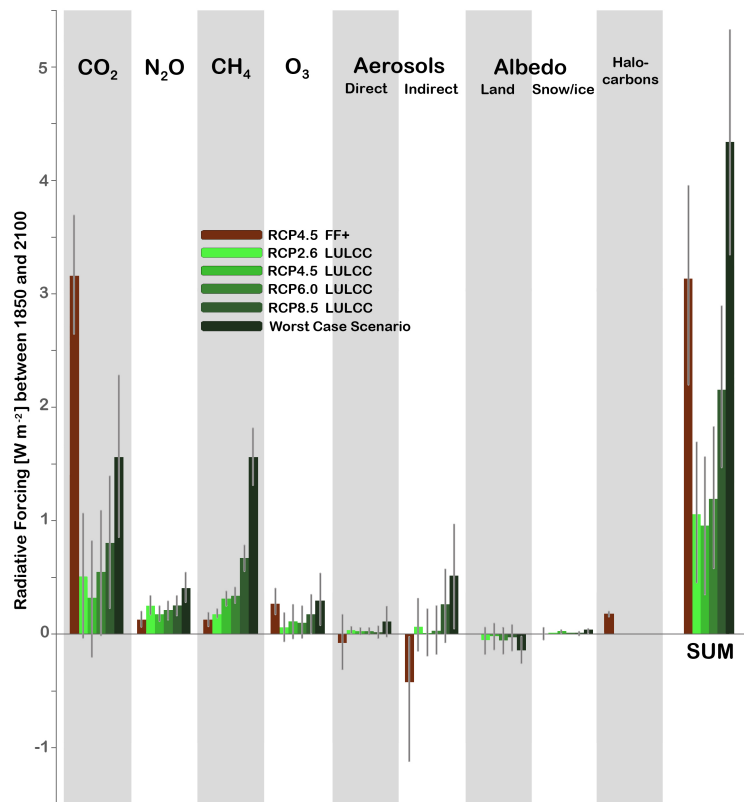


Fig. 6. RF for all LULCC and other anthropogenic impacts (RCP4.5 FF+) estimated by this study for the year 2100, referenced to the year 1850. Error bars show one sigma uncertainties as computed in this study (Table 3). The “SUM” bars show the total RF when all forcing agents are considered.

Potential climate forcing of land use and land cover change

D. S. Ward et al.

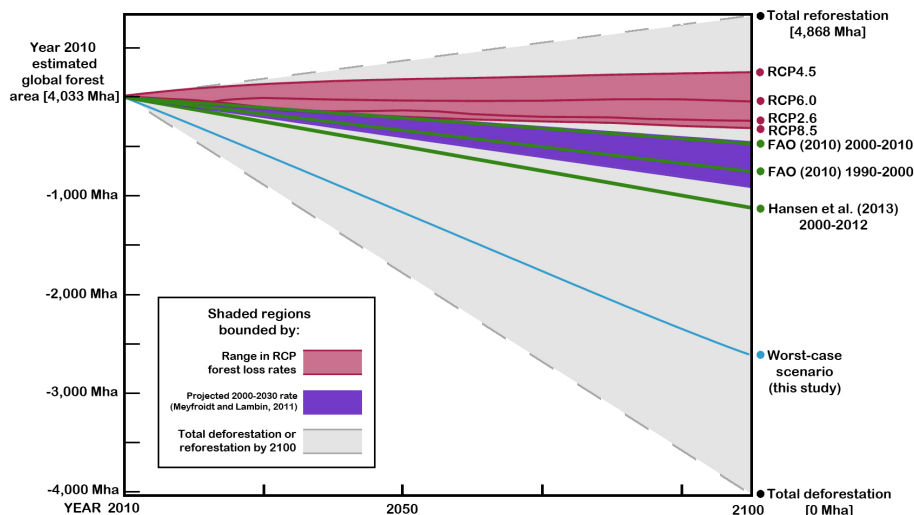


Fig. 7. Comparison of projected annual rates of forest area change. Color lines and shading represent the change in global forest area between 2010 and 2100 for the Representative Concentration Pathways (red) and the worst case scenario (light blue). The grey shaded region is bounded by the annual rate of forest area change required to completely reforest to the estimated prehistoric forest area (Pongratz et al., 2008), or remove all forests by year 2100. Reported and projected forest area change from Meyfroidt and Lambin (2011) (purple), and FAO (2010) and Hansen et al. (2013) (green) are depicted as constant rates through year 2100 to show the result if these rates were sustained.

Title Page

Abstract

Introduction

Conclusions

References

Tables

Figures

⏪

⏩

◀

▶

Back

Close

Full Screen / Esc

Printer-friendly Version

Interactive Discussion